THE BEAM-BEAM INTERACTION

L. R. Evans
CERN, Geneva, Switzerland

1. INTRODUCTION

Particles circulating in a colliding beam storage device like the SPS collider experience a localised focussing field when crossing the opposing beam. To first order this can be approximated by a linear lens which produces a small tune shift from the unperturbed tune, called the linear beam-beam tune shift. However, the force is intrinsically nonlinear and the nonlinearity gives rise to two unwanted effects. Firstly it introduces a dispersion of the tune with amplitude and secondly it excites nonlinear resonances.

The problem of the beam-beam interaction has been of considerable interest for many years. The main reason for this interest is that almost all electron-positron storage rings have fallen short of their design luminosity due to this effect. It is now known that this phenomenon is also a serious limitation in the SPS collider. Although a great deal of theoretical and experimental effort has been invested in the subject, the problem is still not completely understood. There are many theoretical models of the beam-beam interaction and there have been at least two dedicated workshops 1], 2]. In addition, a number of review papers are available 3],4],5].

It is not the object of this paper to try to give another comprehensive review of the subject. Instead, in the rest of this introduction some experimental data on the beam-beam effect in e^+e^- and p-pbar colliders ~~will be~~ presented in order to illustrate their differences and similarities. Then, after treating the linear beam-beam force, the subject of nonlinear resonances ~~will be~~ introduced using some simple examples.* It must be emphasized that these lectures are intended for non-specialists so the normal Hamiltonian treatment will not be used. Instead, the more physically intuitive but also more limiting differential equation method will be employed. This method will be used to investigate one-dimensional beam-beam resonances for a conservative system (hadron colliders only) in the weak-strong régime. The influence of tune modulation and the concept of stochasticity will then be introduced, followed by a short description of the resonance trapping mechanism. Finally, some practical implications for the SPS collider will be discussed.

have
have
* (orig. /HSI)

2. EXPERIMENTAL DATA FROM e^+e^- AND HADRON COLLIDERS

2.1 e^+e^- Colliders

Figure 1 (from reference 6) shows the luminosity versus current observed in the four major e^+e^- colliders operating at the present time. The luminosity L is given by

$$L = \frac{I^2}{4\pi M e^2 f \sigma_x \sigma_y} \qquad (2.1)$$

Where f is the revolution frequency, M. the number of bunches per beam, I the current per beam (assumed equal for the two beams) and $\sigma_{x,y}$ are the standard deviations of the beam size at the crossing point.

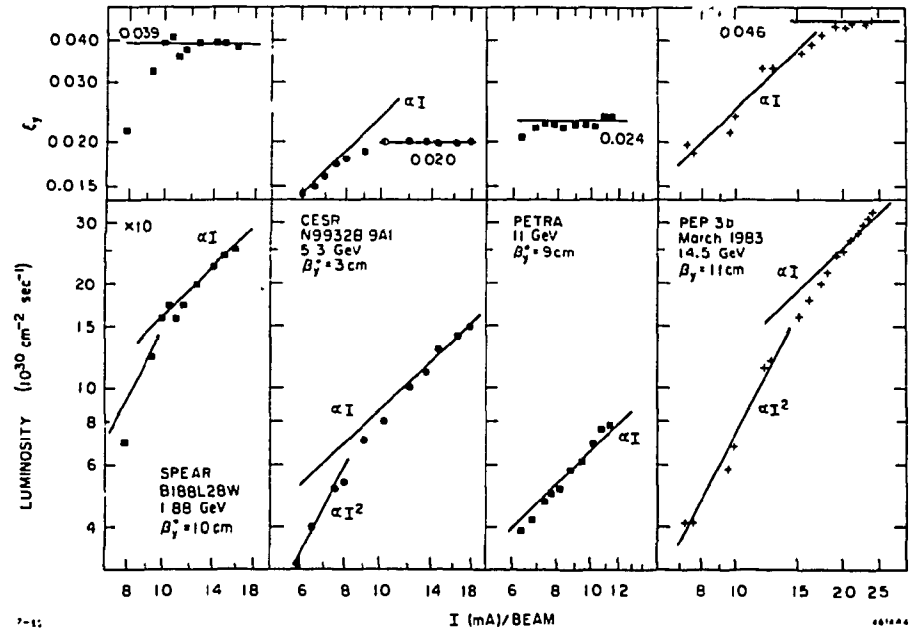

Fig. 1 (from reference 6)

Luminosity and beam-beam tune shift versus current for the four large e^+e^- collider SPEAR, CESR, PETRA and PEP

The behaviour of all four machines is remarkably similar. At low current, except for PETRA, the luminosity increases proportionally to I^2 in agreement with equation 2.1. Above a certain threshold current the curves break and the luminosity is more proportional to I rather than

I^2. Even more clearly the upper plots of the vertical beam-beam tune shift ξ_y as a function of current show a clear saturation above a certain threshold current. This value of the tune shift is generally known as the beam-beam limit and as can be seen from the data it is quite precisely defined for all four machines.

As will be shown later, the vertical tune shift is proportional to the ratio of the current to the vertical beam size and the reason that it saturates is that the beam size increases proportionally with the current above the threshold value. This is an important characteristic of e^+e^- machines. At a given current an equilibrium distribution exists which is a balance between the heating due to the beam-beam interaction and quantum fluctuations and the cooling due to synchrotron radiation damping. The beam size has been observed to blow up by as much as a factor of five before the lifetime is affected 7].

Considerable progress in understanding the dependence of the beam-beam limit on various machine parameters has been made in recent years by the use of computer simulation 8],9],10]. When all the relevant physics is put into the computer programs, results are obtained which closely model the behaviour of real machines. Such simulations have been used in PEP, PETRA and CESR to improve machine performance. The main reason why computer simulation is so successful at modelling e^+e^- machines is that the (non-conservative) particle dynamics needs only to be followed for a few damping times (10^3-10^4 turns) before the equilibrium distribution is established. This is in sharp contrast to the situation in the SPS collider.

2.2 Hadron Colliders

The first hadron collider to operate was the ISR. This is a very special machine for two reasons. Firstly, the operating beam-beam tune shift is very low ($\sim 4 \times 10^{-4}$ per intersection) and is only important in the vertical plane due to the horizontal crossing angle. Secondly, the beams are debunched so except for small effects like intrabeam scattering or power supply ripple, the tune of a given particle remains rigorously constant in time. Under normal operating conditions no important beam-beam effects are observed even though the beams are stacked across relatively low order resonances (7th and 8th order).

In order to achieve a usable luminosity in the SPS collider the beam-beam tune shift must be almost an order of magnitude greater than in the ISR (3×10^{-3} per intersection) and the collisions are head-on so produce equal tune shifts in both planes. In addition, the beams must be bunched as in e^+e^- machines so the tune of a given particle

continuously sweeps through resonances as it performs energy oscillations. However, there is negligible synchrotron radiation damping so an equilibrium distribution does not exist. One would not expect to see a 'hard' beam-beam limit as observed in e^+e^- machines but rather to observe a decay rate of the beam intensity which depends strongly on the current and on the working point.

The important unanswered question before the collider came into operation was whether the decay rate was sufficiently low for useful physics to be done. The required beam lifetime is of the order of a day in order to accumulate enough antiprotons for the next fill. Although the ISR could not answer this question under normal operating conditions, some indication of the magnitude of the effect was obtained in an experiment where the lattice was strongly distorted in order to obtain a beam-beam tune shift of up to 3×10^{-3} per intersection and one of the beams was bunched 11]. The observed bunch lifetime was strongly dependent on the vertical separation between the two beams. The best measured lifetime of 30 hours at least gave some confidence as to the viability of the SPS collider.

Very early in the commissioning period of the collider, strong beam-beam effects were observed 12]. Figure 2 shows a scan of the tune diagram with three proton bunches and a single weak antiproton bunch in the machine (6 crossings per revolution for the antiprotons) and with a beam-beam tune shift of 3.3×10^{-3} per crossing. Figure 2a) shows a chart recorder output of the intensity of one of the proton bunches together with the antiproton bunch on a very sensitive scale. Figure 2b) shows the tune diagram between the third and fourth order resonances, where the 10th, 7th and 11th order resonances are indicated.

The intensity decay rate was measured at different positions in the working diagram indicated by the lines marked 1,2 etc. The meaning of these lines is the following. The proton bunch (with which the tune is measured) has a negligible spread and can be considered to occupy a point in the working diagram which is indicated by the lower point on each line. On the other hand, as we shall see later, the antiprotons have spread in tunes due to the beam-beam interaction. The small amplitude particles are shifted upwards by the total tune spread of $6 \times 0.0033 \approx 0.02$ in each plane, corresponding to the point at the other end of each line. Large amplitude antiprotons occupy most of the space between these two points.

The decay rate of the antiprotons is extremely sensitive to the tune. At the point 1 only the small amplitude antiprotons touch the 10th order resonance and the lifetime (inverse decay rate) is around 300 hours as is

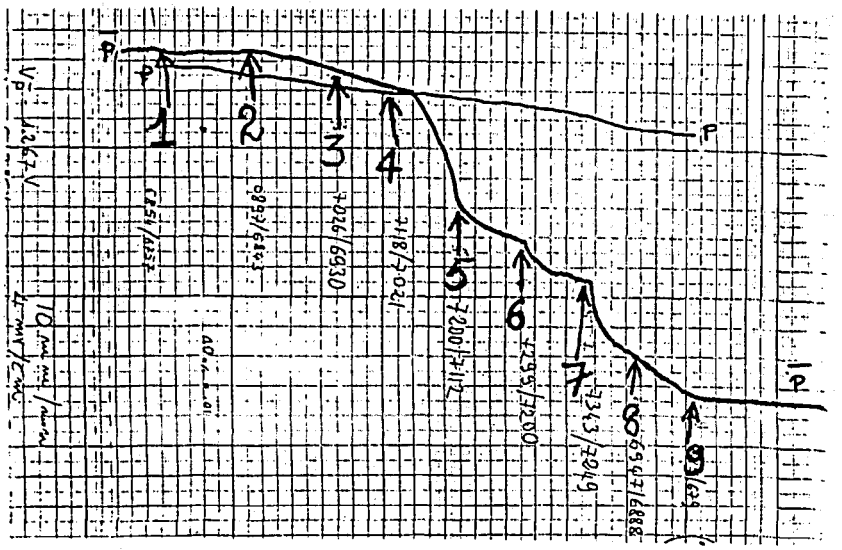

a)

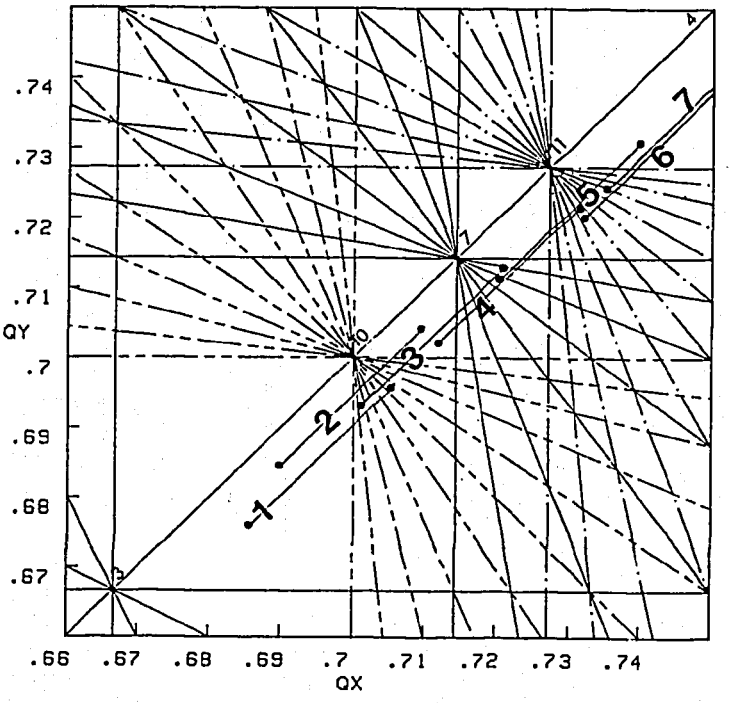

b)

Fig. 2

Scan of the working diagram between the third and fourth order resonances

usual right at the start of storage. As the working point is moved upwards, larger amplitude particles straddle the 10th order resonance (point 2) and the lifetime quickly drops to only 25 hours.

The 7th order resonance (point 4) is extremely destructive, giving a lifetime of only 3 hours. This, at first, is surprising because ideally one would expect the collisions to be exactly head-on, in which case odd order resonances cannot be excited. However, the tune of the antiprotons is different to that of the protons (due to the beam-beam shift) so that the closed orbits are not exactly identical and small displacements of the beam centroids can be expected at the crossing points. In addition, odd order resonances can be driven by the small residual dispersion at the unwanted crossings. Points 6 and 7 show the influence of the 4th order resonance. The lifetime is almost too low to be measurable. Points 8 and 9 show the effect of returning to the initial position (point 1).

The proton decay rate is quite insensitive to the tune. This is because the antiproton beam was too weak to excite beam-beam resonances on the protons and the natural machine nonlinearity for driving resonances of this high order is negligible. The practical implication of all this is that in order to have reasonable conditions for physics the tune must be restricted to a very small region of the working diagram corresponding to that of point 1 in the figure. Therefore the beam-beam effect imposes severe constraints on machine performance.

In contrast to e^+e^- machines, direct computer modelling of the beam-beam interaction is of limited use. The main reason is that there is no equilibrium distribution so that the particle dynamics must be followed for very many turns before a decay rate can be established. In the SPS the antiprotons make something like 10^9 beam-beam collisions per hour and a one-hour lifetime can be considered to be disastrous. Therefore, the computational difficulties are formidable and we are obliged to use simple analytical models like the one developed in the rest of this paper. The real value of simulation programs is to test the models and the approximations that go with them.

3. THE BEAM-BEAM FORCE

We consider a round Gaussian beam with n particles per unit length and with a density distribution

$$\rho(r) = \frac{ne}{2\pi\sigma^2} e^{-r^2/2\sigma^2} \tag{3.1}$$

The Lorenz force on a test particle at a radius r is

$$\underline{F} = e(\underline{E} + \underline{v} \times \underline{B}) = e(E_r \pm \beta c B_\phi).\underline{r} \tag{3.2}$$

where the negative sign corresponds to a particle in the same bunch and the positive sign to a particle in the other beam. $\underline{r}$ is the unit vector.

The radial electric field E_r and the poloidal magnetic induction B_ϕ can be obtained from Gauss' theorem and Ampère's law respectively, neglecting the flux out of the ends of the bunch.

$$2\pi r E_r = \frac{1}{\epsilon_o} \int_0^r 2\pi r' \rho(r') dr'$$

so

$$E_r = \frac{ne}{2\pi r \epsilon_o} (1 - e^{-r^2/2\sigma^2}) \tag{3.3}$$

$$2\pi r B_\phi = \mu_o \int_0^r 2\pi r' \beta c \rho(r') dr'$$

and

$$B_\phi = \frac{ne\mu_o \beta c}{2\pi r} (1 - e^{-r^2/2\sigma^2}) \tag{3.4}$$

Then

$$F_r = \frac{ne^2}{2\pi r \epsilon_o} (1 \pm \beta^2) (1 - e^{-r^2/2\sigma^2}) \tag{3.5}$$

For particles in the same bunch the force falls off as $1/\gamma^2$ and is completely negligible at the energy of the SPS collider. However, this is only the macroscopic effect of the overall space-charge field. Coulomb collisions between individual particles in the same bunch give rise to a phenonmenon called intrabeam scattering which <u>is</u> important in the collider. This effect will not be discussed here.

For particles in the other beam, the effect of electric and magnetic fields is additive. We define an equivalent magnetic field B_{eq} which gives the same force

$$B_{eq} = \frac{F_r}{e\beta c} = \frac{E_r}{\beta c} + B_\phi$$

$$= \frac{ne(1+\beta^2)}{2\pi\,\varepsilon_o\,\beta c\,r}\left(1 - e^{-r^2/2\sigma^2}\right) \qquad (3.6)$$

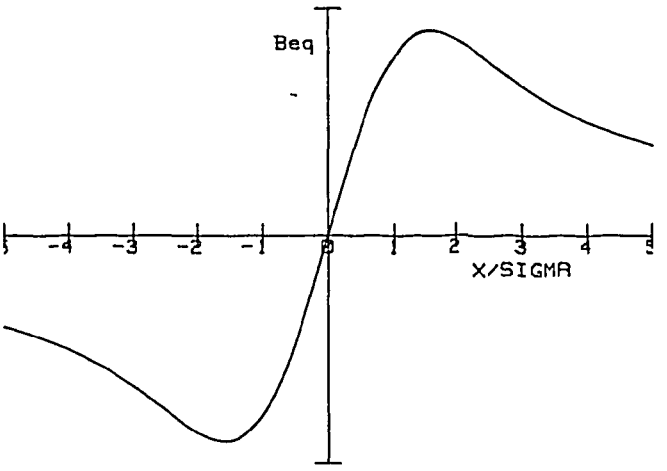

Fig. 3

The equivalent beam-beam field

3.1 The Linear Tune Shift

Small amplitude particles experience an almost linear field with gradient

$$G = \left.\frac{\partial B_{eq}}{\partial r}\right|_{r=0}$$

$$= \frac{ne(1+\beta^2)}{4\pi\,\varepsilon_o\,\beta c\sigma^2} \qquad (3.7)$$

For the SPS collider, $n \simeq 1.6 \times 10^{11}\ m^{-1}$ and $\sigma \simeq 0.1$ mm at the experimental crossing points, giving a gradient of 150 $T.m^{-1}$. The linear tune shift ΔQ_L is given by

$$\Delta Q_L = \frac{1}{4\pi} \cdot \frac{G}{B\rho} \cdot \beta^* \cdot \frac{L}{2} \tag{3.8}$$

where β^* is the beta function at the interaction point and L/2 is the effective length of the interaction (half the bunch length).

Then putting $B\rho = m_o c\beta\gamma/e$ and $r_p = e^2/(4\pi \varepsilon_o m_o c^2)$ we get the linear beam-beam tune shift, which we will call ξ to be compatible with other authors.

$$\xi = \Delta Q_L = \frac{N r_p \beta^*}{4\pi\sigma^2\gamma} \tag{3.9}$$

where N is now the total number of particles per bunch and r_p is the classical proton radius, $r_p = 1.535 \times 10^{-18}$m. We take $\beta = 1$.

In the case of an elliptical beam with Gaussian distribution the tune shift is 13], 14]

$$\xi_{x,z} = \frac{N r_p}{2\pi\gamma\ (\sigma_x + \sigma_z)} \cdot \left[\frac{\beta^*}{\sigma}\right]_{x,z} \tag{3.10}$$

We can write the beam size in terms of the invariant emittance

$$\sigma^2 = \frac{(\epsilon\beta\gamma)\ \beta^*}{4\gamma} \tag{3.11}$$

Equation 3.9 then becomes

$$\xi = \frac{N r_p}{\pi(\epsilon\beta\gamma)} \tag{3.12}$$

so the linear beam-beam tune shift in a hadron machine is independent of the energy and for round beams it is also independent of the beta function at the crossing points. This is why low-beta insertions are so interesting for increasing the luminosity. In the SPS the beta functions at the crossing points are reduced from their normal values of β_H = 50 m, β_V = 50 m, to β_H = 1.3 m, β_V = 0.65 m, giving more than a factor of 50 increase in luminosity but with the same beam-beam tune shift parameter.

If the beam-beam effect only produced a linear tune shift this could easily be corrected by adjusting the overall tune of the machine. However, we see from figure 3 that the field becomes very nonlinear at a modest betatron amplitude and this produces two effects. Firstly, the tune of a particle is a function of the amplitude of its oscillation. Particles with very small amplitude are shifted by the full amount ξ whereas particles with a very large amplitude almost see no effect from the other beam so their tune is not shifted at all. This gives rise to a tune spread inside the beam which cannot be compensated by quadrupoles.

Even more important, it is known that such concentrated nonlinear fields excite resonances and can have a profound influence on the phase space dynamics. The experimental results presented in the previous chapter show a strong dependence of the lifetime of the beam on the tune and bad regions are strongly correlated with 'resonant' values of tune.

In the next sections, the phase space dynamics in the presence of such resonances is investigated. However, since many readers may not be acquainted with the fundamentals of nonlinear resonance theory, a short introduction to the subject is first given with examples using nonlinear driving fields which are somewhat simpler than the beam-beam field.

4. NONLINEAR PHASE SPACE DYNAMICS

We are interested in investigating the perturbed Hill's equation of the form

$$\frac{d^2x}{ds^2} + K(s)x = g(x,s) \tag{4.1}$$

where $g(x,s)$ is some driving function nonlinear in amplitude x and distributed in azimuthal position s.

The above equation can be transformed into the equation of the perturbed harmonic oscillator using the classic transformation of Courant and Snyder 15].

$$\eta = X/\sqrt{\beta} \quad ; \quad \theta = \int ds/Q\beta.$$

Since $Q\beta = R$, in this 'smooth' approximation, θ changes by 2π per revolution. Equation 4.1 then becomes

$$\frac{d^2\eta}{d\theta^2} + Q^2\eta = Q^2\beta^{3/2}g(\eta,\theta) \tag{4.2}$$

The most elegant and general way of investigating the behaviour of such a system is using Hamiltonian dynamics. For a complete treatement of the problem using this method the reader is referred to the literature 16],17]. In the present work a more physically transparent, although less powerful method is used in which the discussion will be limited to one-dimensional motion only.

The homogeneous equation

$$\eta'' + Q^2\eta = 0 \tag{4.3}$$

gives a first integral

$$(\eta'/Q)^2 + \eta^2 = c^2 \tag{4.4}$$

The trajectories in the phase space η, η'/Q are circles of radius c. The area of the circle is $\pi c^2 = \pi\varepsilon$, where ε is the "emittance" of a particle i.e. the area of phase space (divided by π) enclosed by the particle trajectory.

The solution of equation 4.3 is

$$\begin{aligned}\eta(\theta) &= \sqrt{\varepsilon}\cos(Q\theta + \phi)\\ &= \sqrt{\varepsilon}\cos\Phi\end{aligned} \tag{4.5}$$

were ε and ϕ are <u>constants</u> defined by the initial conditions.

4.1 <u>The Amplitude and Phase Equation</u>

In order to solve the inhomogeneous equation 4.2 we use the method of Kryloff and Bogoliubov, often called the method of variation of constants or variation of parameters (for a detailed discussion see reference 18]).

We assume now that ε and ϕ are no longer constants but we allow them to vary slowly with θ.

$$\eta = \sqrt{\epsilon}\ \cos\Phi \qquad a)$$
$$\eta' = -Q\sqrt{\epsilon}\ \sin\Phi \qquad b) \tag{4.6}$$

where in the second equation we already neglect the ϵ' and ϕ' terms.

The variables ϵ and Φ are nearly the action/angle variables of Hamiltonian dynamics. The true canonical variables are generally called I and Φ, where $I = \epsilon Q/2$.

The inverse transformation is

$$\epsilon = \eta^2 + (\eta'/Q)^2 \qquad a)$$
$$\Phi = -\arctan(\eta'/Q\eta) \qquad b) \tag{4.7}$$

Differentiating 4.7 a) we get

$$\begin{aligned}\frac{d\epsilon}{d\theta} &= 2\eta\eta' + \frac{2\eta'\eta''}{Q^2} \\ &= \frac{2\eta'}{Q^2}(\eta'' + Q^2\eta) \\ &= 2\eta'\beta^{3/2}g(\eta,\theta)\end{aligned} \tag{4.8}$$

Similarly from 4.7 b) we get

$$\begin{aligned}\frac{d\Phi}{d\theta} &= -\left[\frac{Q(\eta\eta'' - \eta'^2)}{Q^2\eta^2 + \eta'^2}\right] \\ &= Q - \frac{Q\beta^{3/2}g(\eta,\theta)\eta}{\epsilon}\end{aligned} \tag{4.9}$$

The second term in equation 4.9 is just the tune shift due to the perturbation.

Finally we substitute the unperturbed solution 4.6 into the right hand sides of the above equations to get the two important equations for the amplitude and phase

$$\frac{d\epsilon}{d\theta} = 2Q\beta^{3/2}\epsilon^{1/2}\, g(\sqrt{\epsilon}\ \cos\Phi, \theta)\sin\Phi \qquad a)$$
$$\frac{d\Phi}{d\theta} = Q - \frac{Q\beta^{3/2}g(\sqrt{\epsilon}\ \cos\Phi, \theta)\cos\Phi}{\sqrt{\epsilon}} \qquad b) \tag{4.10}$$

We will now illustrate the use of these equations with the help of some simple examples.

4.2 A Single Octupole

We consider a single short octupole of length L and strength $K = (\partial^3 B_z/\partial X^3)/6\ B\rho$.

The driving term in equation 4.2. is then of the form

$$g(\eta,\theta) = K\beta^{3/2}\eta^3 f(\theta) \tag{4.11}$$

and the θ dependence can be expressed as a Fourier expansion

$$f(\theta) = \frac{L}{\pi Q\beta}\left[\frac{1}{2} + \sum_{p=1}^{\infty} \cos p\,\theta\right] \tag{4.12}$$

Then 4.10 gives

$$\frac{d\epsilon}{d\theta} = \frac{2KL}{\pi} \cdot \epsilon^2\beta^2 \cos^3\Phi \sin\Phi \left[\frac{1}{2} + \sum_{p=1}^{\infty} \cos p\,\theta\right] \quad \text{a)}$$

$$\frac{d\Phi}{d\theta} = Q - \frac{KL}{\pi}\epsilon\beta^2 \cos^4\Phi \left[\frac{1}{2} + \sum_{p=1}^{\infty} \cos p\,\theta\right] \quad \text{b)} \tag{4.13}$$

For the time being, we will neglect the second term in the square brackets on the grounds that it is rapidly oscillating so that its contribution over many revolutions averages to zero. Later on, we will analyse the situation when this is not the case.

The phase equation is then

$$\frac{d\Phi}{d\theta} = Q - \frac{KL}{2\pi}\epsilon\,\beta^2 \cos^4\Phi \tag{4.14}$$

where the second term is the perturbation of the tune due to the octupole. The $\cos^4\Phi$ term shows that the instantaneous tune depends on the amplitude of the particle on any particular traversal of the lens. What we are interested in is the mean tune over many revolutions. If there are no resonance effects the particle will have sampled the octupole

over a large number of phases between 0 and 2π after many revolutions. So to find the mean tune we average over the $\cos^4\Phi$ term.

$$\overline{\frac{d\Phi}{d\theta}} = Q - \frac{KL}{2\pi} \cdot \varepsilon\beta^2 \cdot \frac{1}{2\pi} \int_0^{2\pi} \cos^4 \Phi \, d\Phi$$

$$= Q - \frac{3KL\ \varepsilon\ \beta^2}{16\pi} \qquad (4.15)$$

$$= Q - \frac{B''' L\beta\ x^2}{32\pi\ B\ \rho}$$

The second term is the well-known expression for the variation of tune with amplitude in an octupole. It is used to good advantage to stabilise high-intensity beams against transverse instabilites by providing Laudau damping through a spread of betatron frequencies as a function of emittance. As we will see later, it also plays a crucial rôle in influencing the phase space trajectories of particles in the presence of beam-beam induced resonances. We will call it the nonlinear detuning ΔQ_{NL}. Note that if we had taken a sextupole instead of an octupole as an example, we would have an integral over $\cos^3\Phi$ which would have given no nonlinear detuning.

Averaging the amplitude equation 4.10 a) in the same way gives

$$\overline{\frac{d\varepsilon}{d\theta}} = \frac{KL\varepsilon^2\beta^2}{\pi} \cdot \frac{1}{2\pi} \int_0^{2\pi} \sin \Phi \cos^3\Phi d\Phi$$

$$= 0 \qquad (4.16)$$

so the octupole has no effect on the amplitude of oscillation. The phase space trajectories are still circles but the tune depends on emittance.

We now wish to analyse the conditions under which we cannot neglect the second term in brackets in equation 4.13. In 4.13 b) we have terms of the form $\cos^4\Phi \cos p\theta$. Firstly we expand the term $\cos^4\Phi$ using well-known trigonometric identities.

$$\cos^4 \Phi = \frac{\cos 4\Phi}{8} + \frac{\cos 2\Phi}{2} + \frac{3}{8} \qquad (4.17)$$

and we see that we have the nonlinear detuning immediately from equation 4.13 b) without needing to do the averaging trick, due to the constant term in the above expansion. Of course, all we have done is to expand $\cos^4 \phi$ as a Fourier series and the factor 3/8 is just the zeroth

harmonic.

Then

$$\cos^4 \Phi \cos p\theta = \frac{1}{16} (\cos (4\Phi + p\theta) + \cos (4\Phi - p\theta)) + \frac{1}{4} (\cos (2\Phi + p\theta) + \cos (2\Phi - p\theta)) + \frac{3}{8} \cos p\theta \qquad (4.18)$$

Slowly varying terms appear in the above expression when one of the difference terms is close to zero. This happens when

$$Q = p/4$$

or

$$Q = p/2$$

These values of the tune correspond to the 4th order and half-integer resonances. We will now investigate the phase space trajectories when the tune is in the vicinity of such resonant values. It will be noticed that the half integer resonance, which is normally associated with a quadrupole perturbation, can also be driven by an octupole perturbation. In general, a resonance of order n can be driven by <u>all higher multipoles</u>. The significance of this statement will become apparent when we discuss beam-beam resonances.

In the phase and amplitude equations we now keep the resonant term $\cos(4\Phi - p\theta)$ (assuming that the tune is near to a 4th order resonance) as well as the nonlinear detuning term to get

$$\frac{d\epsilon}{d\theta} = \frac{KL\beta^2}{8\pi} \cdot \epsilon^2 \sin 4\psi$$

$$\frac{d\Phi}{d\theta} = Q + \Delta Q_{NL} + \frac{KL\beta^2}{16\pi} \epsilon \cos 4\psi \qquad (4.19)$$

where $\psi = (Q - p/4)\theta + \phi$ is called the "slow" phase variable.

4.3 <u>The Resonant Invariant</u>

It is left to the reader to show that the amplitude and phase equations near a resonance of order n are

$$\frac{d\epsilon}{d\theta} = 2n\epsilon^{n/2} B_n \sin n\psi \qquad a)$$

$$\frac{d\psi}{d\theta} = (Q - p/n) + n A_n \epsilon^{n/2-1} + n B_n \epsilon^{n/2-1} \cos n\psi \qquad b) \tag{4.20}$$

The nonlinear detuning is

$$\Delta Q_{NL} = n A_n \epsilon^{n/2-1} \tag{4.21}$$

and the resonance (half) width is

$$\Delta Q_n = n B_n \epsilon^{n/2-1} \tag{4.22}$$

We will see later the physical significance of the resonance width. In general, if the resonance is driven by an arbitrary azimuthal distribution of multipoles the Fourier decomposition 4.12 must be done more carefully, taking into account the variation of strength and beta function at the individual elements. In general, for M arbitrarily spaced short lenses

$$A_n = \frac{1}{2^{n+1} \pi \, (n/2)!^2} \sum_{i=1}^{M} \frac{B_i^{n-1} L_i}{B\rho} \beta_i^{n/2} \tag{4.23}$$

and

$$B_n = \sqrt{a_p^2 + b_p^2} \tag{4.24}$$

where

$$a_p = \frac{1}{2^n . \pi . n!} \sum_{i=1}^{M} \frac{B_i^{n-1} L_i}{B\rho} \cdot \beta_i^{n/2} \cos p\,\theta_i \tag{4.25}$$

$$b_p = \frac{1}{2^n . \pi . n!} \sum_{i=1}^{M} \frac{B_i^{n-1} L_i}{B\rho} \beta_i^{n/2} \sin p\,\theta_i \tag{4.26}$$

and

$$B^{n-1} = \frac{d^{n-1}B_y}{dx^{n-1}}$$

From the amplitude and phase equations 4.20 we can derive an important invariant Multiplying 4.20a) by $d\psi/d\theta$ and 4.20b) by $d\varepsilon/d\theta$ and subtracting, we get

$$\frac{d}{d\theta}\left[(Q - p/n)\, \varepsilon + 2A_n\, \varepsilon^{n/2} + 2B_n\, \varepsilon^{n/2} \cos n\psi \right] = 0 \qquad (4.27)$$

$$(Q - p/n)\varepsilon + 2A_n\varepsilon^{n/2} + 2B_n\varepsilon^{n/2} \cos n\psi = \text{Constant} \qquad (4.28)$$

Equation 4.28 gives us the trajectories of particles in the variables ε,ψ in the vicinity of a resonance of order n. Once the initial conditions ε_o and ψ_o fix the values of the constant the motion can then be followed for all time using equation 4.28.

These trajectories are influenced by both the resonance excitation and the nonlinear detuning. The octupole example we considered above excites both of these terms. In order to illustrate separately the influence of excitation and detuning, in the next sections we will consider the example of a single sextupole which we have already shown produces no nonlinear detuning. Then by adding a zeroth harmonic octupole term we will show how the trajectories are modified.

The resonant invariant is

$$(Q - p/3)\varepsilon + 2\,\varepsilon^{3/2}B_3 \cos 3\psi = C \qquad (4.29)$$

Consider the situation exactly on resonance when $Q-p/3 = 0$. Then for values of $\cos 3\psi = 0$ particles must go to infinite amplitude. The whole of the phase space is open. (Figure 4a)).

Slightly off resonance we have

$$\Delta Q_L \varepsilon + 2\varepsilon^{3/2}B_3 \cos 3\,\psi = C \qquad (4.30)$$

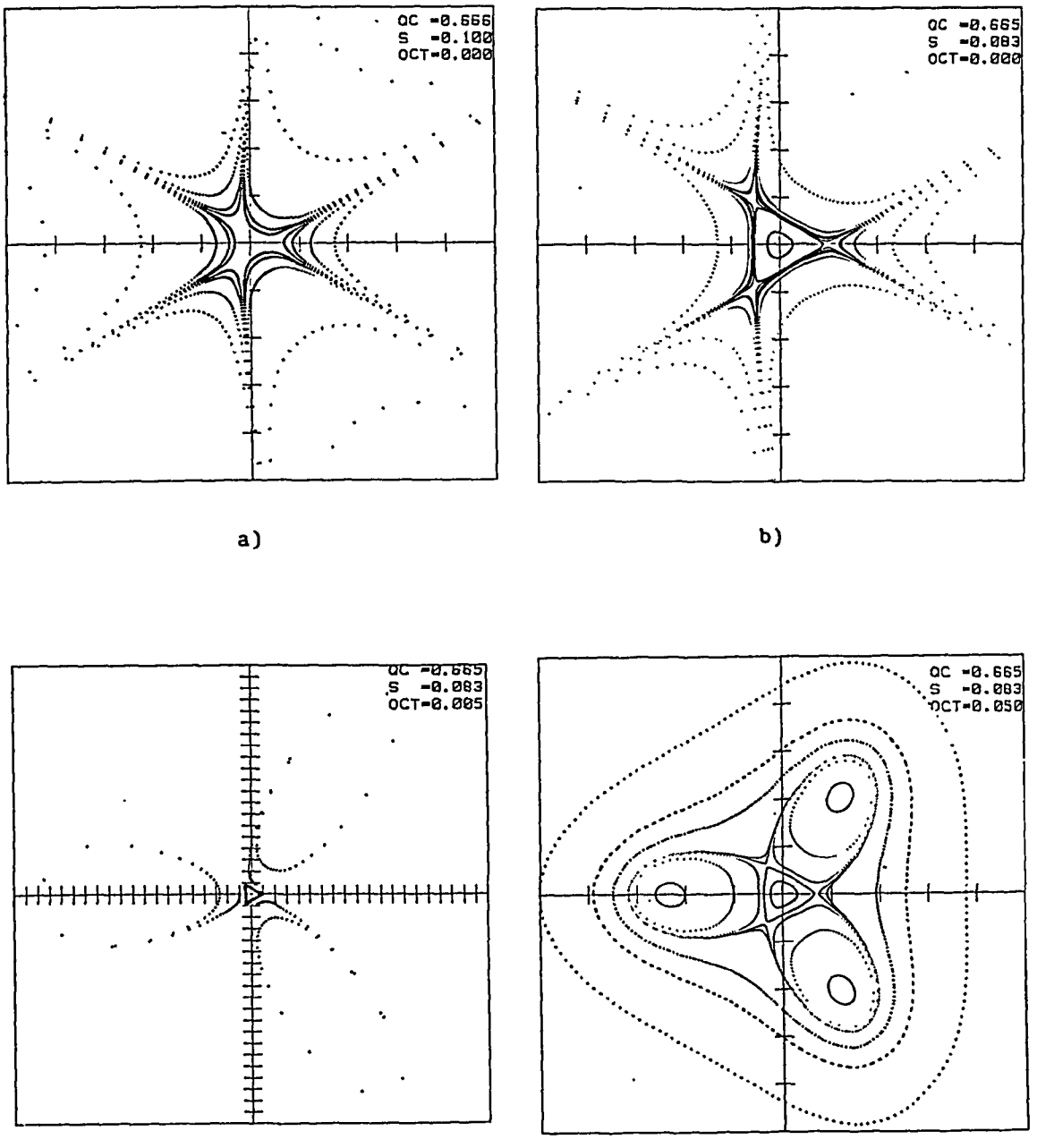

Fig. 4

Phase space trajectories in the vicinity of a 3rd order resonance without (a) and b)) and with (c) and d)) octupole stabilisation.

where $\Delta Q_L = Q - p/3$, the distance of the linear tune from the resonant value.

We now observe the appearance of fixed points $d\epsilon/d\theta = 0$, $d\psi/d\theta = 0$, giving $\sin 3\psi = 0$, $\cos 3\psi = \pm 1$ and $\Delta Q_L = 3\epsilon_f^{3/2} B_3$

where ϵ_f is the fixed point amplitude. One fixed point is the origin around which small amplitude particles move on circular trajectories. It is called a stable fixed point. The other three fixed points at $\psi = 0$, $2\pi/3$, $4\pi/3$ are unstable fixed pointed and define a separatrix between closed and open trajectories. (Figure 4b)).

The tune shift corresponding to the fixed point is called the resonance width ΔQ_3.

$$\Delta Q_3 = 3\epsilon_f^{1/2} B_3$$

$$= \frac{\beta^{3/2}\epsilon^{1/2} L}{16\pi B\rho} \cdot \frac{\partial^2 B}{\partial x^2} \qquad (4.31)$$

A particle with emittance ϵ_f will find itself inside the separatrix and stable if $\Delta Q_L > \Delta Q_3$ but outside the separatrix and consequently unstable if $\Delta Q_L < \Delta Q_3$. Therefore ΔQ_3 is smallest distance from the resonant tune for a particle with emittance ϵ_f to remain stable. This concept of resonance width is useful for low-order unstabilised resonances but is frequently misused in the context of high order resonances in the presence of nonlinear detuning as is the case for beam-beam resonances.

The third-integer resonance is frequently used to obtain a slow spill of particles from a synchrotron. As the tune is slowly pushed towards the resonance particles stream out through the unstable fixed points making bigger and bigger jumps in amplitude each revolution until they finally cross a thin-wire electrostatic septum and are extracted from the machine.

4.4 The Nonlinear Detuning

We conclude this chapter with a short discussion of the influence of nonlinear detuning on the phase space trajectories. Since the tune depends on the amplitude the effect is to stabilise the trajectories in as much as amplitude growth of particles on resonance leads to a tune change which tends to move the particles off resonance.

As an example, consider the effect of switching on an octupole lens in the vicinity of the sextupole resonance already discussed.

Thus

$$\Delta Q_L \epsilon + \frac{K\epsilon^2}{2} + 2\,\epsilon^{3/2} B_3 \cos 3\psi = C \qquad (4.32)$$

Figures 4c) and 4d) illustrate the effect of increasing octupole strength in stabilising the resonance. With a weak octupole the trajectories spiral back in as the octupole changes the large amplitude tune. Stronger octupole completely stabilises the phase space. Stable and unstable fixed points appear about which the particles move in closed (elliptical) or open (hyperbolic) orbits.

The nature of the fixed points can be investigated by making a small amplitude expansion around the fixed points. The phase and amplitude equations written in terms of the radius $r = \epsilon^{1/2}$ are, in the general case of a resonance of order n

$$\frac{dr}{d\theta} = nr^{n-1} B_n \sin n\psi \qquad a)$$
$$\frac{d\psi}{d\theta} = \Delta Q_L + Kr^2 + n\,B_n\,r^{n-2} \cos n\psi \qquad b) \qquad (4.33)$$

At the fixed points $r = r_o$ then $dr/d\theta = d\psi/d\theta = 0$. Putting $r = r_o + \Delta r$, $\psi = \psi_o + \Delta\psi$. Then

$$\frac{d\Delta r}{dr} = n^2\,B_n r_o^{n-1} \cos n\psi_o\,\Delta\psi \qquad a)$$
$$\frac{d\Delta\psi}{d\theta} = (2Kr_o + n(n-2)\,B_n\,r_o^{n-3} \cos n\psi_o)\,\Delta r \qquad b) \qquad (4.34)$$

with $\cos n\psi_o = \pm 1$.

Then

$$\Delta r'' = n^2 B_n r_o^{n-1} \cos n\psi_o (2Kr_o + n(n-2)B_n\,r_o^{n-3} \cos n\psi_o)\,\Delta r \qquad (4.35)$$

and neglecting the second term in brackets we obtain

$$\Delta r'' - 2B_n K n^2 r_o^n \cos n\psi_o \Delta r = 0 \qquad (4.36)$$

which is the harmonic oscillator equation if $B_n K \cos n\psi_o < 0$, giving circular orbits around the fixed point or hyperbolic orbits if $B_n K \cos n\psi_o > 0$.

The unstable fixed points define separatrices. The stable fixed points are the centres of islands of stability into which particle orbits becomes locked. The stability of the large amplitude pnase space depends on the relative strength of the resonant excitation to nonlinear detuning.

The sextupole example illustrated above requires a supplementary octupole lens to stabilise the resonance. However, the beam-beam force itself provides both nonlinear detuning and resonance excitation. The next step will be to investigate the phase space topology for this case using the method developed above.

5. BEAM-BEAM RESONANCES

In this section we will analyse the one-dimensional particle motion for the strong-weak case. This means that we are interested in the behaviour of a weak beam under the influence of a strong beam in which the particle trajectories remain circles in phase space. That is to say we do not take into account the perturbation of the strong beam by the weak beam. This approximation is probably good for the present operating parameters of the SPS collider, where the beam-beam tune shift due to the antiprotons is almost an order of magnitude smaller than that due to the protons.

The object is to solve the amplitude and phase equations 4.10 using the beam-beam field 3.6. Assuming the beam-beam kick to be located over a small distance L the driving term is

$$g(\eta,\theta) = \frac{8\xi\sigma^2}{Q\eta\beta^{5/2}}\left[1 - e^{-\beta\eta^2/2\sigma^2}\right]\left[\frac{1}{2} + \sum_{p=1}^{\infty} \cos p\theta\right] \qquad (5.1)$$

Substituting the unperturbed solution $\eta = \sqrt{\varepsilon}\cos\Phi$ in this equation, we obtain the phase equation

$$\frac{d\Phi}{d\theta} = Q - \frac{4\xi}{\alpha}\left[1 - e^{-\alpha \cos^2\Phi}\right]\left[\frac{1}{2} + \sum_{p=1}^{\infty} \cos p\theta\right] \qquad (5.2)$$

where $\alpha = \varepsilon\beta/2\sigma^2$.

Now the next step is to extract the slowly varying part of equation 5.2. This can be done in two ways.

Expanding the exponential we get

$$\frac{1}{\alpha}(1 - e^{-\alpha \cos^2\Phi}) = \sum_{n=1}^{\infty}\left[\frac{(-1)^{n-1}\alpha^{n-1}}{n!}\right]\cos^{2n}\Phi \tag{5.3}$$

and using the expansion

$$\cos^{2n}\Phi = \frac{1}{2^{2n}}\left[\sum_{\ell=0}^{n-1}\frac{2n!\ 2\cos(2(\ell-n)\Phi)}{(2n-\ell)!\ \ell!} + \frac{(2n)!}{(n!)^2}\right] \tag{5.4}$$

We obtain the phase equation as a triple summation

$$\frac{d\Phi}{d\theta} = Q - 4\xi\left[\sum_{m=1}^{\infty}\frac{(-1)^{m-1}\alpha^{m-1}}{2^{2m}\ m!}\sum_{\ell=0}^{m-1}\left\{\frac{2.(2m)!\cos(2(\ell-m)\Phi)}{(2m-\ell)!\ \ell!} + \frac{(2m)!}{(m!)^2}\right\}\right] \cdot\left[\frac{1}{2} + \sum_{p=1}^{\infty}\cos p\theta\right] \tag{5.5}$$

The task is now to extract the slowly varying part of this expression. The DC term is easy. It is

$$\Delta Q_{NL} = \xi\sum_{m=1}^{\infty}\left[\frac{(-1)^{m-1}(2m!)\alpha^{m-1}}{2^{2m-1}\ (m!)^3}\right] \tag{5.6}$$

This is just the variation of tune with amplitude but now as well as the octupole term all the higher multipoles of the beam-beam force are important.

The slow term in cos nψ is more difficult to spot because the resonance of order n is also driven by all the higher multipoles of the beam-beam force. We are interested in terms of the form cos(pθ - 2(ℓ - m)Φ) where

$$p\theta - 2(\ell - m)Q\theta \simeq 0 \tag{5.7}$$

i.e.

$$Q = \frac{p}{2(m - \ell)}$$

$$= p/n \tag{5.8}$$

where n is the order of the resonance. Therefore we can get rid of the summation over ℓ by keeping only the terms for which

$$\ell = m - n/2 \tag{5.9}$$

The slowly varying part of equation 5.5. transforming to the slow phase ψ is then

$$\frac{d\psi}{d\theta} = (Q - p/n) + \xi\, U'(\alpha) + \xi\, V'_n(\alpha) \cos n\psi \tag{5.10}$$

where

$$U'(\alpha) = Q_{NL}/\xi \qquad \text{a)}$$

and

$$V'_n(\alpha) = \sum_{m=n/2}^{\infty} \frac{(-1)^{m-1}\alpha^{m-1}(2m!)}{2^{2m-2}m!.(m + \frac{n}{2})!(m - \frac{n}{2})!} \qquad \text{b)} \tag{5.11}$$

The function $V'_n(\alpha)$ can be identified as the equivalent of the 'resonance width' for a beam-beam resonance. The infinite sum is simply the consequence of the fact that a resonance of order n is driven by all higher multipoles 19]. This is very important at large amplitude where the strength decreases instead of increasing monotonically as is the case for magnet imperfection resonances.

Closed form solutions for these functions can be obtained by averaging over the phase variable 20], 21]. The nonlinear detuning can be obtained by averaging the zeroth harmonic term in equation 5.2.

$$U'(\alpha) = \frac{1}{\pi\alpha} \int_0^{2\pi} (1-e^{-\alpha \cos^2\phi})\, d\phi \tag{5.12}$$

giving

$$U'(\alpha) = \frac{2}{\alpha} \left[1 - e^{-\alpha/2} I_0(\alpha/2)\right] \tag{5.13}$$

The resonant term can be obtained by putting $p\theta = n\psi - n\phi$ and averaging the coefficient of the term in cos $n\psi$

$$V_n'(\alpha) = \frac{2}{\pi\alpha} \int_0^{2\pi} (1 - e^{-\alpha \cos^2\phi}) \cos n\phi \, d\phi \tag{5.14}$$

giving

$$V_n'(\alpha) = (-1)^{\frac{n}{2}+1} \cdot \frac{4}{\alpha} \cdot e^{-\alpha/2} I_{\frac{n}{2}}(\alpha/2) \tag{5.15}$$

The expressions 5.13 and 5.15 are identical with the series 5.6 and 5.11. The nonlinear detuning and resonance width functions are shown in figures 5 and 6. For centred beams only even order resonances are driven. Small orbit displacements between the beams at the crossing points will also drive odd order resonances. The nonlinear detuning and resonance width functions for these resonances can be derived easily by introducting an orbit offset in equations 5.12 and 5.14. However, since no new physics is introduced into the problem these resonances will be ignored in what follows.

A similar argument can be used to obtain the amplitude equation

$$\frac{d\alpha}{d\theta} = n\xi \, V_n(\alpha) \sin n\psi \tag{5.16}$$

and finally the resonant invariant can be obtained.

$$C = (Q - p/n)\alpha + \xi U(\alpha) + \xi \, V_n(\alpha) \cos n\psi \tag{5.17}$$

which gives us the phase space trajectories. Notice that the linear tune shift ξ is just a scaling parameter affecting both resonance strength and nonlinear detuning.

The important question is whether the large amplitude phase space is stable or unstable. Figures 7a and 7b) show some typical trajectories in the vicinity of half integer and 4th order resonances. The island structure with stable and unstable fixed points is clearly visible. The fixed point amplitude is given by

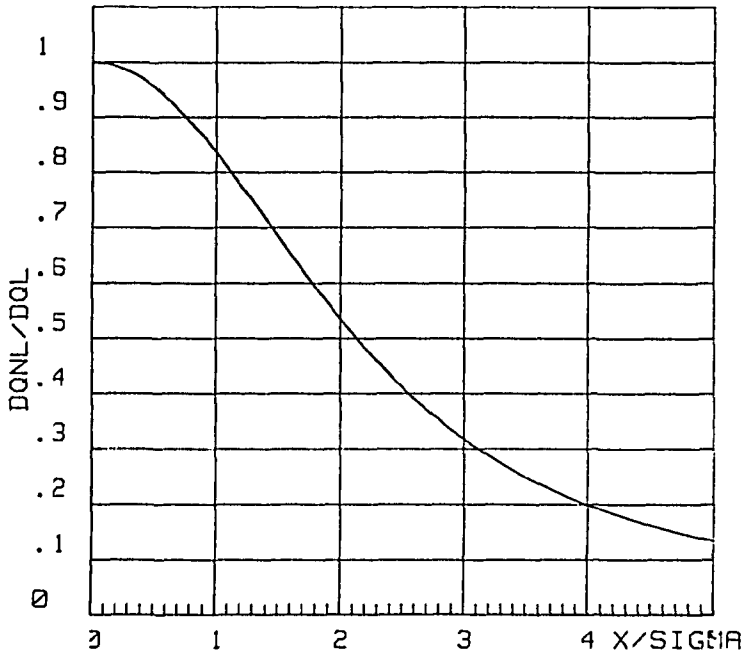

Fig. 5

The nonlinear detuning function $U'(\alpha)$ with $\alpha = X^2/2\sigma^2$.

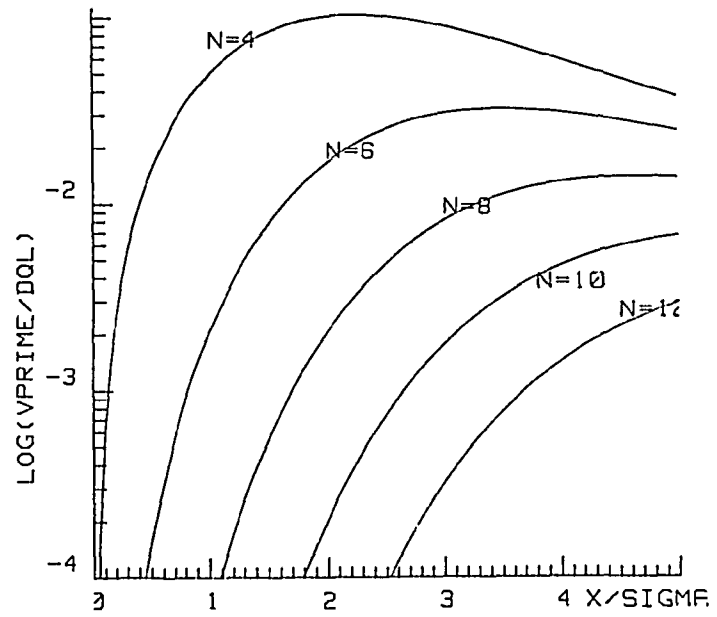

Fig. 6

The "Resonance Width" function $V'_n(\alpha)$

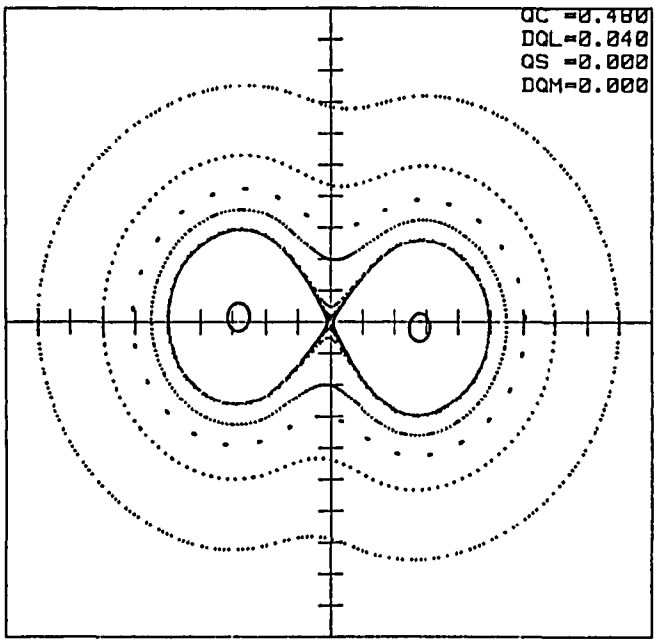

a)

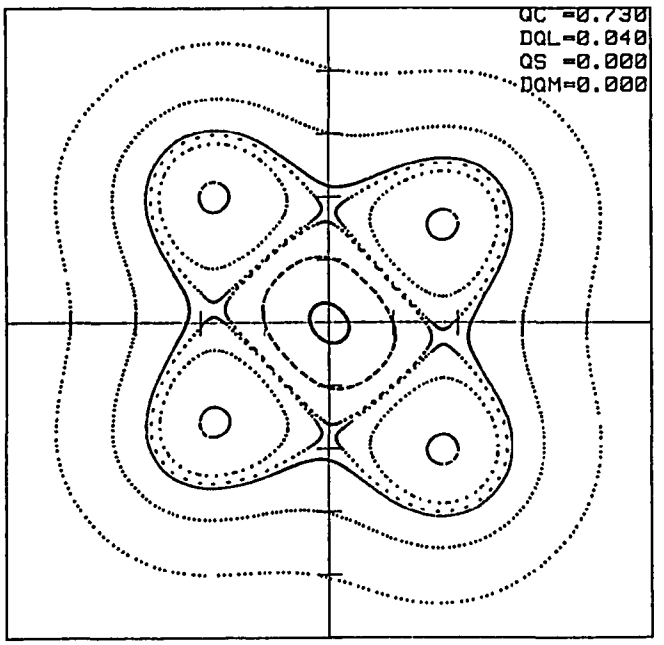

b)

Fig. 7

Phase space trajectories in the vicinity of the half-integer (a)) and 4th order (b)) beam-beam resonances.

$$\frac{d\alpha}{d\theta} = \frac{d\psi}{d\theta} = 0$$

giving $\cos n\psi = \pm 1$

and

$$(Q - p/n) + \xi\, U'(\alpha_f) \pm \xi\, V'_n(\alpha_f) = 0 \qquad (5.18)$$

The resonant term $\xi V_n'(\alpha_f)$ is generally small and can be neglected to first approximation. The island amplitude is then given by

$$Q + \xi\, U'(\alpha_f) = p/n \qquad (5.19)$$

Now $Q + \xi u'(\alpha)$ is simply the tune of a particle with amplitude α, so an island structure appears at an amplitude where the particle tune is resonant.

The phase space is stable. This in an important characteristic of beam-beam resonances. The nonlinear detuning produced by the beam-beam force itself is always sufficient to stabilise the resonance. Therefore, there is no mechanism to explain the observed beam behaviour with single static one-dimensional resonances. This is in obvious contradiction with our practical experience so there is clearly something missing in the model.

5.1 Tune modulation

In order to maximise the luminosity in the SPS collider the beams are bunched. Consequently, the particles perform energy oscillations and there are several mechanisms by which these oscillations can result in a tune modulation. The most important of these are:

- Non-zero chromaticity

In order to stabilise the dense bunches against coherent instabilities the chromaticity must be adjusted to be slightly positive. This results in a tune modulation at the synchroton frequency f_s.

- Non-zero dispersion at the crossing points.

The SPS low-beta insertions are designed to give zero dispersion at the two experimental crossing points. However, with 3 bunches per beam in the machine, collisions occur at 4 other crossings where the dispersion is not zero (~ 0.2m). If the number of bunches per beam is doubled, as is

required to reach design luminosity the beams will collide also in the arcs where the dispersion is even bigger (~ 1 m). This gives rise to a modulation of the closed orbit of the test particle with respect to the strong beam centroid and results in both a modulation of the strength of the beam-beam kick and to the exictation of odd order resonances. It is intended to eliminate this effect in the future by separating the beams at the unwanted crossings with electrostatic deflectors.

- Variation of arrival time

Energy oscillations cause a modulation of the longitudinal position of a particle in the bunch. Since the beta function varies through the crossing point there is a modulation of both the strength of the beam-beam force (for flat beams) and of the phase at which a test particle sees the beam-beam kick. This phase modulation results in a tune modulation which is known to be important in e^+e^- machines with short bunches and small beta values at the crossing points. Appropriate calculations and computer simulations 22] have shown that this effect is small for the SPS.

Whatever the mechanism of the tune modulation the result is that particles continually sweep across resonances and one might expect that this will have an important influence on the phase space trajectories. In the next section, in order to investigate the effect of tune modulation we abandon for the moment the mathematical model and instead turn to the computer.

5.2 Computer Simulation

We would like to simulate the particle orbits in the presence of tune modulation of the form $Q = Q_o + \hat{Q} \sin Q_s\theta$ where Q_s is the synchrotron tune defined as the ratio of the synchrotron frequency to the revolution frequency. We simulate the particle motion by a linear transformation around the supposedly linear machine followed by a delta-function nonlinear beam-beam kick.

The beam-beam kick is

$$\Delta x' = - \frac{8\pi \xi \sigma^2}{x \beta^*} (1 - e^{-x^2/2\sigma^2}) \qquad (5.20)$$

Transforming to new variables $\bar{x} = x/\sigma$. $\bar{x}' = \beta^* x'/\sigma$ we get the position and angle of a particle on turn n + 1 from its coordinates on turn n

$$X_{n+1} = X_n \cos 2\pi Q_n + X'_n \sin 2\pi Q_n$$

$$X'_{n+1} = - X_n \sin 2\pi Q_n + X'_n \cos 2\pi Q_n - \frac{8\pi\xi}{X_{n+1}} \left(1 - e^{-X^2_{n+1}/2}\right) \qquad (5.21)$$

$$Q_{n+1} = Q_o + \hat{Q} \sin (2\pi Q_s n).$$

where the tune is modulated at the frequency Q_s. This kind of transformation is generally called a nonlinear mapping.

In the next sections we will investigate the phase space topology under such a mapping in the vicinity of the 6th order beam-beam resonance, which has been chosen to clearly illustrate the physics rather than for any practical purpose. In reality we know that such a low order resonance would be extremely destructive. The phase space maps are shown in the form of coloured plates which for technical reasons cannot be ideally placed in the text, so the indulgence of the reader is solicited.

As a reference, plate 1a) shows the 6th order resonance under static tune conditions. The 6 islands are clearly visible and the whole phase space is stable.

These phase space trajectories have been generated by plotting the position of selected 'seed' particles each revolution. Plate 1b) shows the effect of introducing tune modulation into the picture. The same seed particles as in the previous example are used. The smooth trajectories previously observed now seem to have broken up into diffuse bands which could be interpreted as the onset of 'stochastic' behaviour. However, if we change the time scale of our observation we will see that this is far from being the case. Plate 2a) shows the trajectories of the same seed particles but now plotted once per synchrotron period instead of once per revolution period. We observe the appearance of a beautifully ordered multiple-island structure where 4th, 6th, 8th and 10th order resonances can be picked out.

5.3 Synchrobetatron Resonances

To understand where these islands come from we have to resort to the theory. The slowly varying part of the phase equation was obtained by expanding the terms of the form $\cos n\Phi \cos p\Theta$ and keeping the slowly varying part $\cos(n\Phi - p\Theta)$.

Now the phase Φ is modulated since

$$\Phi = \int Q d\theta = \Phi_o - (\hat{Q}/Q_s) \cos Q_s\theta \tag{5.22}$$

Then

$$\cos n\Phi = \cos(n\,\Phi_o - (n\hat{Q}/Q_s) \cos Q_s\theta) \tag{5.23}$$

and using the well-known identity

$$\cos(A + B \cos C) = \sum_k J_k(B) \cos (A + kC) \tag{5.24}$$

we get

$$\cos (n\phi) = \sum_k J_k (n\hat{Q}/Q_s) \cos (n\phi_o + kQ_s\theta) \tag{5.25}$$

The product $\cos n\Phi \cos p\theta$ then gives slow terms of the form $\cos(n\Phi_o + kQ_s\theta - p\theta)$ which in turn gives the resonance condition.

$$Q = p/n + k\,Q_s/n, \qquad -\infty < k < \infty \tag{5.26}$$

The main resonance at $Q = p/n$ is therefore split into freqency modulated sidebands spaced by Q_s/n and reduced in strength by the factor $J_k(n\hat{Q}/Q_s)$. These sideband resonances are called <u>synchrobetatron resonances.</u>

We can now understand the multiple island structure observed in Plate 2a). A ring of islands forms whenever the tune obeys equation 5.26. The large amplitude (or unperturbed) tune Q_o is 0.651 whereas small amplitude particles are shifted by the full beam-beam tune shift to 0.681. Islands form at amplitudes corresponding to the following tune values.

$3/4 - 3Q_s/4$	$= 0.675$
$4/6$	$= 0.666$
$5/8 + 3Q_s/8$	$= 0.6625$
$7/10 - 4Q_s/10$	$= 0.660$

with $Q_s = 0.1$.

5.4 Stochasticity

We have seen that tune modulation increases the density of resonances but we have not yet found any evidence of unstable or 'stochastic' behaviour. In the previous example the islands are well separated and the separatrices are clean and well defined. However, as the linear tune shift increases so does the slope of the nonlinear detuning function and the islands are pushed closer and closer together. Plates 2 to 4 show the effect of gradually increasing the linear tune shift when the tune modulation amplitude and frequency are kept constant. The large amplitude tune is chosen in all cases so that the 4/6 resonance lies at an amplitude at approximately 2σ.

In Plate 2b) the tune shift has been increased to 0.04 and we see that the sidebands of the 6th and 8th order resonance move closer together although the separatrices are still clearly defined. Increasing the tune shift to 0.05 (Plate 3a) we observe the appearance of a sideband of the 14th order resonance as well as the first sideband of the 6th order resonance at large amplitude . The trajectories in the vicinity of the separatrix of the 8th order resonance become diffuse and degenerate into a stochastic band.

Increasing the tune shift further (Plate 3b), we clearly start to see the break-up of the separatrices. Stable islands can still be observed but their size is reduced and the stochastic bands become wider. Finally, (Plate 4a) shows the large-scale break-up of the phase space. The islands now become isolated from one another by wide stochastic regions through which particles diffuse to large amplitude. In addition, a complicated high order substructure can be observed around the islands.

As shown in the above examples, stochastic behaviour is observed when the separatrices of different resonances touch each other. There exists a very well known criterion for the onset of stochasticity called the Chirikov criterion 23] which states that the phase space becomes unstable when the width of resonances exceeds their separation. For a clear discussion of the Chirikov criterion applied to accelerators, the reader is referred to Tennyson 24] and Courant 25]. Physically the stochastic limit signifies the randomisation of particle phases between successive resonance crossings 12].

It should be noted that it is not necessary to introduce tune modulation to drive a system to the stochastic limit. For example, Plate 4b) illustrates the phase space for the same conditions as Plate 4a) but without tune modulation. The sidebands disappear and consequently the

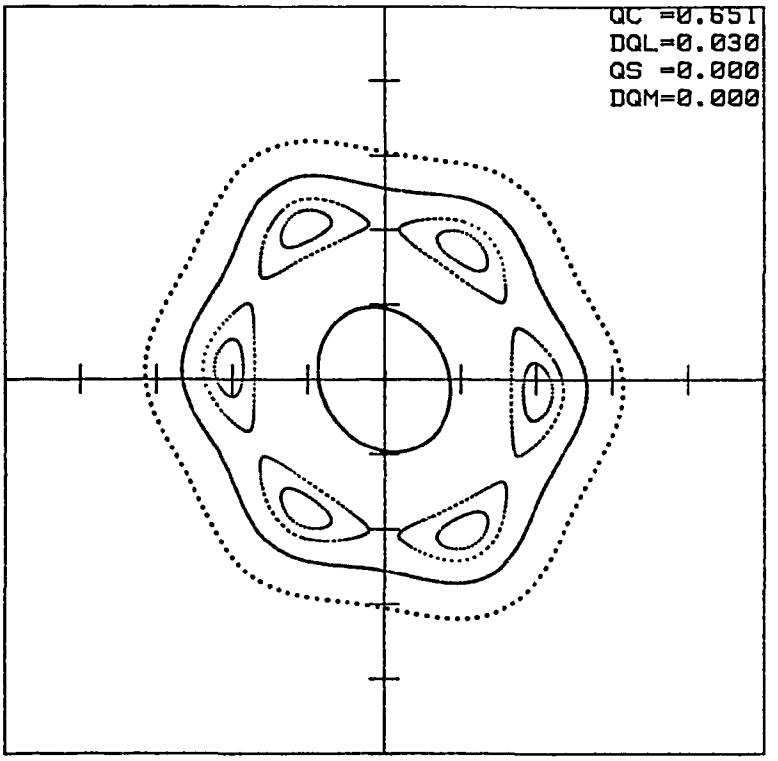

Plate 1a

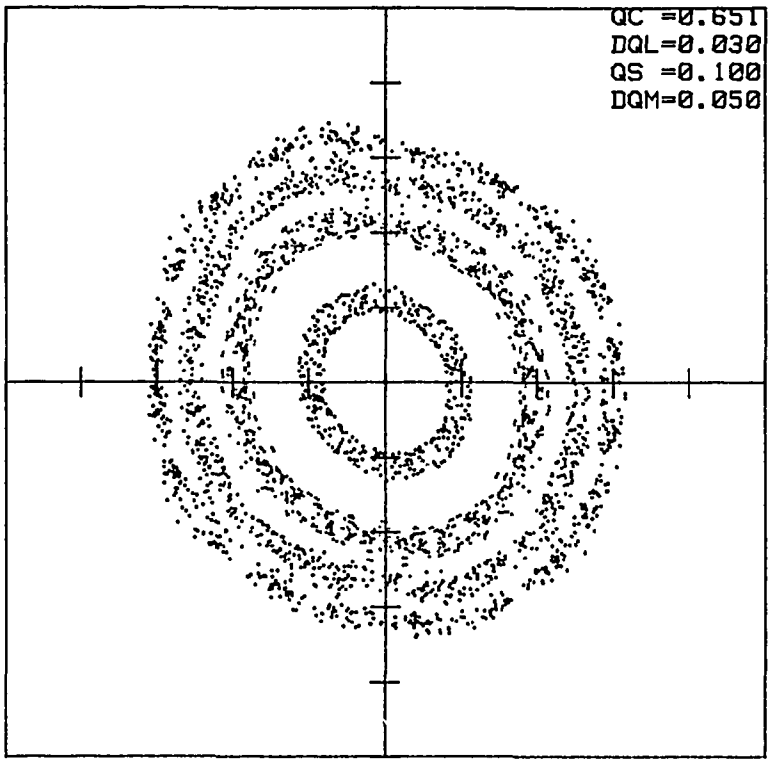

Plate 1b

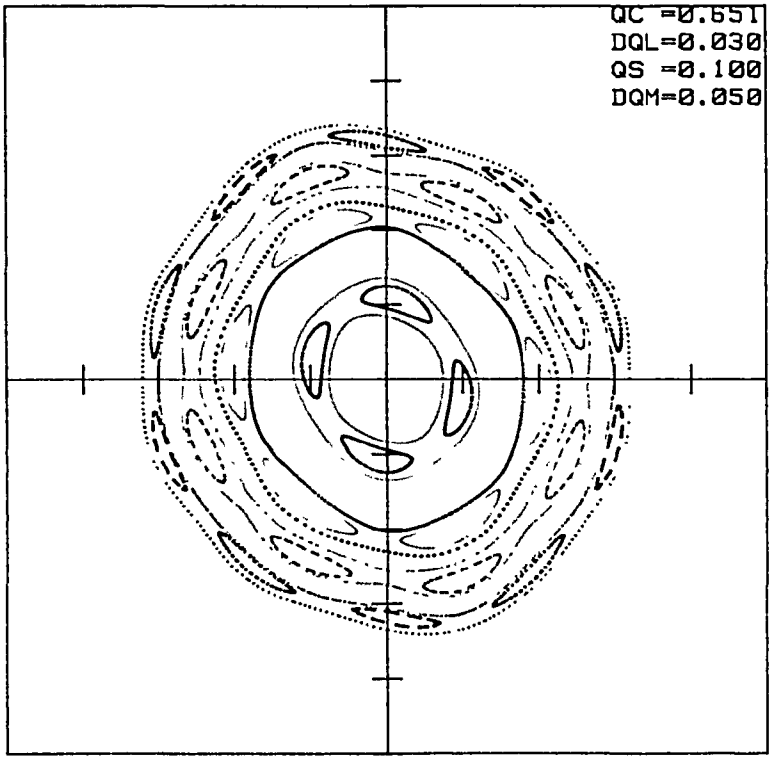

Plate 2a

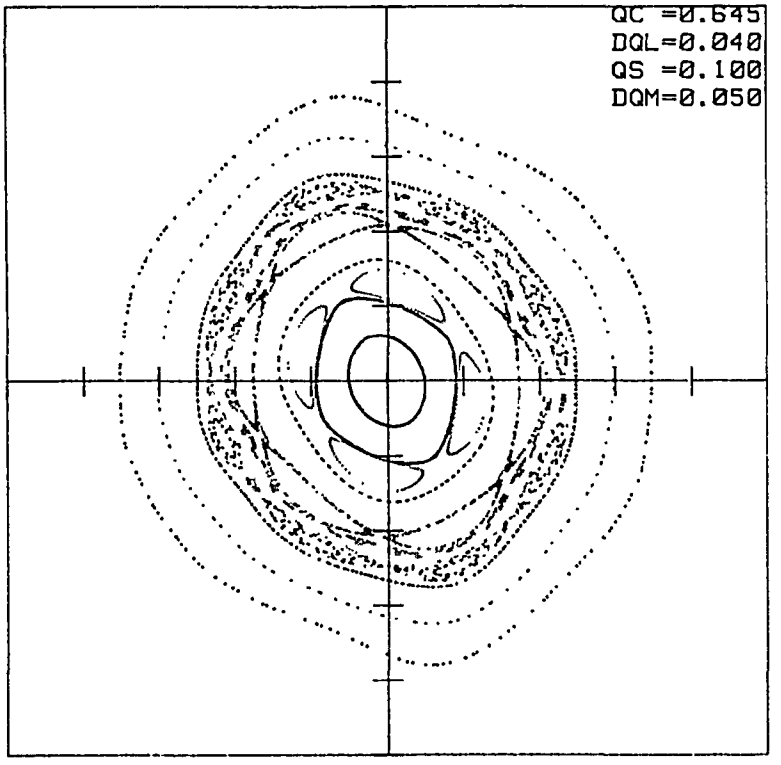

Plate 2b

trajectories are perfectly ordered. However, one may observe a resonance of 14th order at large amplitude, well separated from the main 6th order resonance. Clearly if the tune shift is increased substantially, these resonances would move closer together and other resonances would appear. At large enough tune shift the system would again become stochastic as in the previous example, but to do this the tune shift would need to be a sizeable fraction of an integer.

The effect of tune modulation, then, is to enormously increase the density of resonances and thereby reduce the Chirikov threshold.

5.5 Approximate Calculation Of the Stochasticity Threshold

In the above examples the parameters have been chosen to produce strong effects in order to illustrate the principle of resonance overlap and the effect of the synchrotron sidebands. If the true beam-beam limit for the antiprotons would really be around 0.07 on a 6th order resonance, the beam-beam effect would be no limitation at all. In reality the synchrotron tune is very much smaller than 0.1 and consequently the synchrotron sidebands are much closer together. Computer simulation under conditions appropriate to a real machine has proved to be enormously difficult mainly because, even under bad conditions the beam lifetime is of the order of hours during which time a particle makes of the order of 10^9 beam-beam interactions.

In this chapter, instead of pursuing the numerical approach any further we attempt to compute an approximate threshold for stochastic motion using our one-dimensional model. We consider a machine with M beam-beam interactions per revolution.

When calculating the resonant invariant we must now be careful to carry out the correct Fourier decomposition of the driving term. The invariant is now of the form

$$C = (Q - p/n)\alpha + \Gamma\, U(a) + \bar{\Gamma}\, V_n(\alpha) \cos n\Psi \qquad 5.27)$$

Γ is just the total tune spread

$$\Gamma = M\xi \qquad 5.28)$$

where we have assumed that the tune shift is the same at all intersections i.e. equal bunch intensities.

$\bar{\Gamma}$ is the Fourier coefficent of the pth azimuthal harmonic

$$\bar{\Gamma} = \xi \left[\left(\sum_{i=1}^{M} \cos p\,\theta_i \right)^2 + \left(\sum_{i=1}^{M} \sin p\theta_i \right)^2 \right]^{1/2} \qquad (5.29)$$

Electron-positron machines are usually designed with a high superperiodicity in order to eliminate as many as possible of the Fourier harmonics 5.29. Computer simulation and practical experience 7] have shown that small machine imperfections such as a difference in the phase advance between the intersections or spurious dispersion at the interaction points strongly affect the machine performance. Consequently a considerable effort is made to correct these errors.

On the other hand, the SPS collider has no supersymmetry at all. The two low-beta insertions are in two adjacent straight sections. All resonances are excited more or less strongly and for any given machine the Fourier coefficients 5.29) can be calculated from the theoretical lattice. However, these coefficients are enormously sensitive to small lattice perturbations especially in view of the high order of the harmonics of interest (p = 277 for a 10th order resonance). Therefore, in what follows we assume that the successive kicks are distributed at more or less random phase. The expection value of $\bar{\Gamma}$ is then just $\xi M^{1/2}$.

The width of an island can be computed with reference to figure 8.

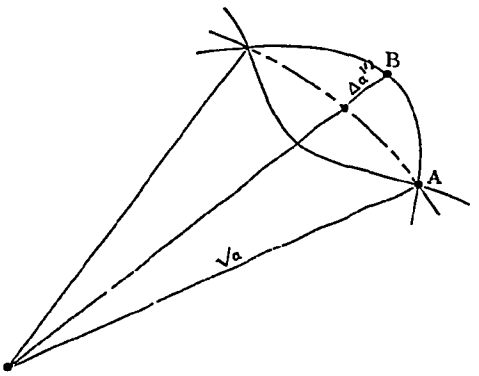

Fig. 8

Consider the unstable point A. The invariant is

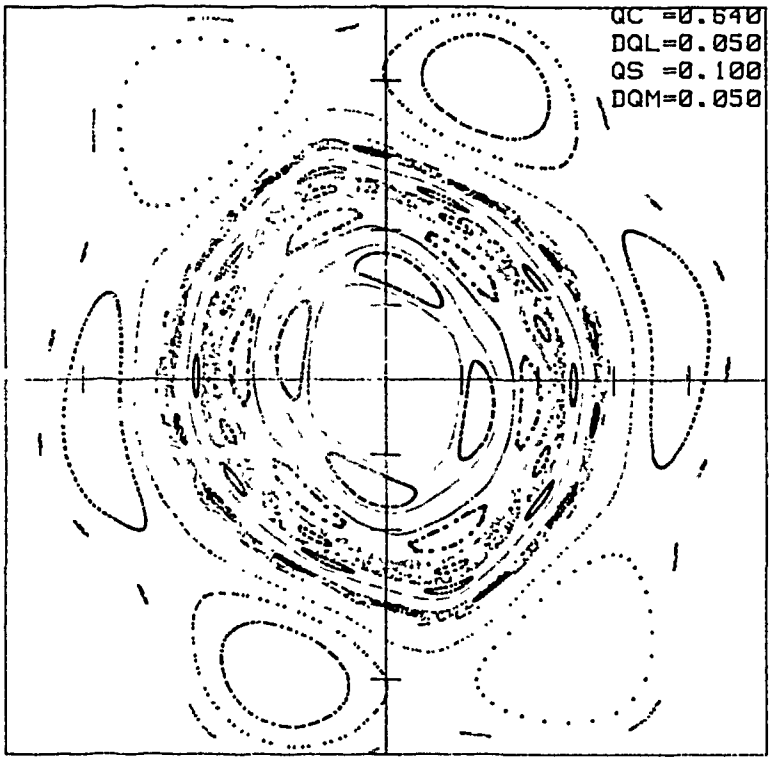

Plate 3a

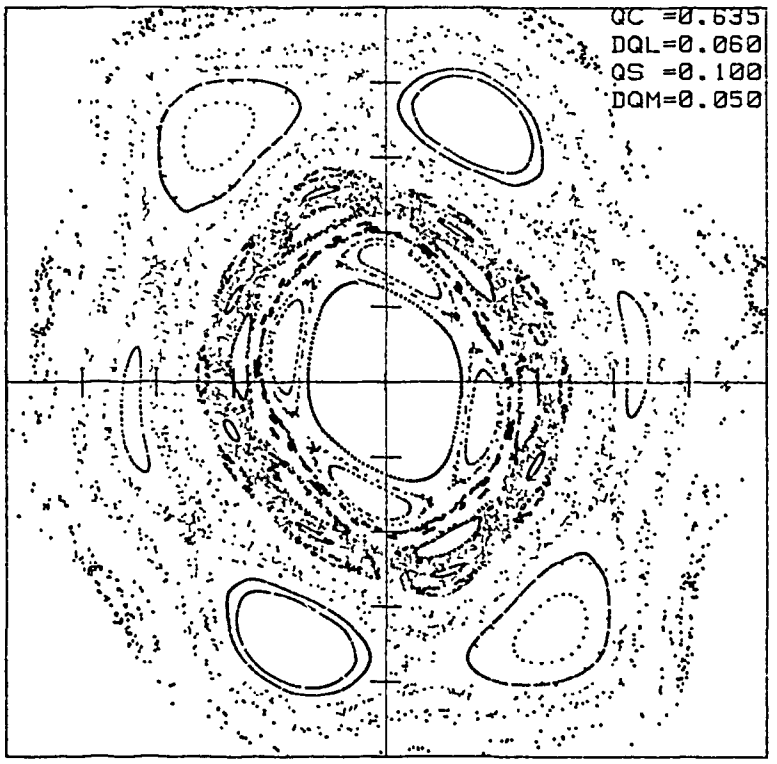

Plate 3b

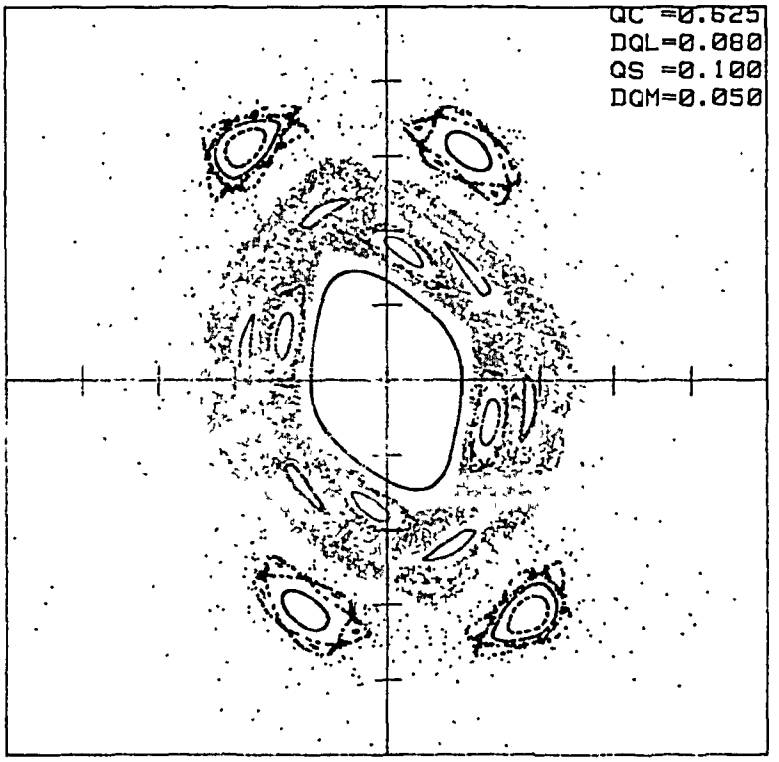

Plate 4a

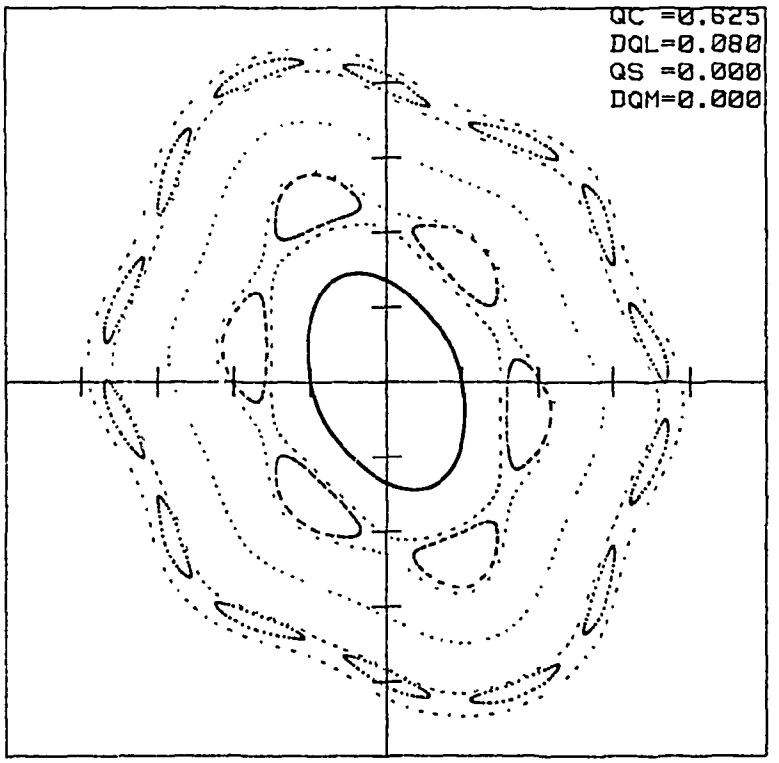

Plate 4b

$$C_F = (Q - p/n)\alpha_f + \Gamma\, u(\alpha_f) + \bar{\Gamma}\, Vn\ (\alpha_f) \qquad 5.30)$$

Moving around the separatrix to B

$$C_F = (Q - p/n)\alpha + \Gamma\, u(\alpha) - \bar{\Gamma}\, V_n(\alpha)) \qquad 5.31)$$

Subtracting 5.30 from 5.31

$$(Q - p/n)\Delta\alpha + \Gamma(u(\alpha) - u(\alpha_F)) - \bar{\Gamma}(V_n(\alpha) + V_n(\alpha_F) = 0 \qquad 5.32$$

Expanding $U(\alpha)$ and $V_n(\alpha)$ around α_f

$$(Q-p/n)\Delta\alpha + \Gamma(U'(\alpha_f)\Delta\alpha + U''(\alpha_f)\Delta\alpha^2/2) - \bar{\Gamma}(2V_n(\alpha_f) + \Delta\alpha\, V_n'\ (\alpha_f)) = 0 \qquad (5.33)$$

But,

$$d\psi/d\theta = (Q - p/n) + \Gamma U'(\alpha_f) - \bar{\Gamma}\, V_n'\ (\alpha_f) = 0 \qquad (5.34)$$

Therefore

$$\Delta\alpha = 2\sqrt{\frac{\bar{\Gamma}\, V_n\ (\alpha_f)}{\Gamma\, U''\ (\alpha_f)}} \qquad (5.35)$$

Remembering that the kth sideband is weakend by the factor $J_k(n\hat{Q}/Qs)$ and putting $\Gamma = \xi M$, $\bar{\Gamma} = \xi M^{1/2}$ the width of the island in α is

$$\text{width} = 2\Delta\alpha$$

$$= 4\sqrt{\frac{V_n\ (\alpha)\ J_k(n\hat{Q}/Q_s)}{\sqrt{M}\ U''\ (\alpha)}} \qquad (5.36)$$

Notice that the island width is independent of the linear tune shift. However, the island separtion is not. The separation in tune is

$$\Delta Q = Q_s/n = M \xi U''(\alpha) \Delta\alpha \tag{5.37}$$

so

$$\Delta\alpha = \frac{Q_s}{nM \xi U'' (\alpha)} \tag{5.38}$$

Equating 5.36 and 5.38 we get the Chirikov threshold for resonance overlap in terms of the beam-beam tune shift

$$\xi = \frac{Q_s}{4nM} \sqrt{\frac{M^{1/2}}{U''(\alpha)\ V_n(\alpha)\ J_k(n\hat{Q}/Q_s)}} \tag{5.39}$$

Let us take the case of a 10th order resonance in the SPS collider. We use the following parameters.

$$Q_s = 4 \times 10^{-3};\ \hat{Q} = 1.5 \times 10^{-3};\ n = 10;\ M = 6;\ k = 0$$

The following table gives the threshold tune shift for stochastic behaviour as a function of amplitude.

x/σ	α	$u''(\alpha)$	$V_{10}(\alpha)$	ξ
2	2	0.138	9.4×10^{-5}	1.1×10^{-2}
3	4.5	0.053	2.2×10^{-3}	3.8×10^{-3}
4	8	0.031	1.3×10^{-2}	2.0×10^{-3}

Table 1

We see from the table that at least for the large amplitude particles the theoretical tune shift for stochastic behaviour is not too far from the operating tune shift in the SPS where we know that these particles have a bad lifetime. Considering the many simplifying assumptions the agreement can be considered to be reasonable. In the real world many other effects such as coupling or noise will conspire to reduce this threshold.

5.6 Diffusion Rate

We would now like to address the question of the influence of the synchrotron frequency on beam loss rate in the stochastic region, which signifies a randomisation of the betatron phase between resonance crossings but tells us nothing about the rate of emittance growth .

From the amplitude equation 5.16, the change of emittance due to a single resonance crossing is 16]

$$\int_{\alpha_1}^{\alpha_2} \frac{d\alpha}{V_n(\alpha)} = \int_{\theta_1}^{\theta_2} n \bar{\Gamma} \sin n\psi \, d\theta \tag{5.40}$$

The procedure for performing the integral on the right hand side is well known 16]. It gives

$$\int_{\alpha_1}^{\alpha_2} \frac{d\alpha}{V_n(\alpha)} = n \bar{\Gamma} \sqrt{\frac{2\pi}{n|dQ/d\theta|}} \tag{5.41}$$

We assume that the change in α per crossing is very small so that the variation of $V_n(\alpha)$ can be ignored.

Then

$$\Delta\alpha = n \bar{\Gamma} V_n(\alpha) \sqrt{\frac{2\pi}{n|dQ/d\theta|}} \tag{5.42}$$

and the change in radius $r = \alpha^{1/2}$ is then

$$\Delta r = \bar{\Gamma} V_n(\alpha) \sqrt{\frac{\pi n}{2\alpha|dQ/d\theta|}} \tag{5.43}$$

Treating the emittance change as a random-walk process, the change in the mean square radius after N crossings is then

$$\overline{\Delta r^2} = \frac{N}{2} (\Delta r)^2 \tag{5.44}$$

Putting $|dQ/d\theta| = 2\hat{Q}\, Q_S/\pi$ and $N = 2Q_S f_r t$

then

$$\overline{\Delta r^2} = \left[\frac{\pi^2 \Gamma^2 V_n^2(\alpha)\, n\, f_r}{4\,\alpha\,\hat{Q}} \right] t$$

$$= 4\,D\,t \qquad (5.45)$$

where D is a diffusion coefficient, given by

$$D = \frac{\pi^2 M \xi^2 V_n^2(\alpha)\, n\, f_r}{16\,\alpha\,\hat{Q}} \qquad (5.46)$$

The important point here is that D is independent of the synchrotron frequency so as long as the motion is stochastic, the diffusion rate is independent of the frequency of modulation. This stochastic régime was recognized by Schoch 16] as the régime of 'fast random crossings'.

In the above analysis we have observed the particle motion on a time scale of which the unit of time is the synchrotron period and we have ignored what happens in between. In the next chapter we will investigate the limit of very low modulation frequency when the sideband picture breaks down and we need to look more carefully at the details of the motion within the synchrotron period.

5.7 Resonance trapping

Figure 9 shows a superposition of instantaneous "snapshots" of the phase space as the unperturbed tune is changed from 0.615 in steps of 0.01. We see clearly the islands of the 6th order resonance which move to larger amplitude and expand in area as the tune changes. Now the question is what happens if this tune change is made so slowly that it is done adiabatically? In this case, particles initially captured in the stable islands at small amplitude will move with the islands to larger amplitude so long as the adiabaticity condition is satisfied. This mechanism is closely analogous to the processs of adiabatic capture and stacking in synchrotron space and it forms the basis of the resonance trapping model of Chao and Month 26]. Obviously, as the tune modulation direction reverses the islands contract and retrace their original paths finally transporting the particles back to their starting points. However, if in the course of the movement the island amplitude exceeds the dynamic

aperture of the machine or if the adiabaticity conditions are violated, particle loss can result.

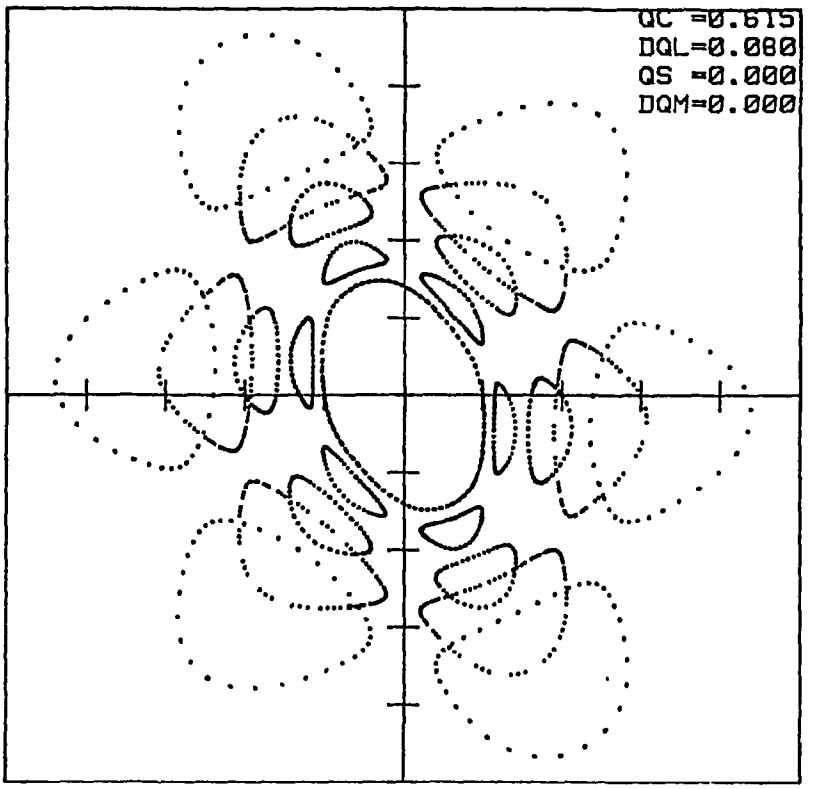

Fig. 9

Instantaneous 'snapshots' of the phase space topology near a 6th order beam-beam resonance as the tune is changed from 0.615 (inner islands) to 0.645 in steps of 0.01.

The important question is what is the critical modulation frequency below which the motion can be considered to be adiabatic? This has been analysed in detail for beam-beam resonances 27], and can be calculated using the nonlinear detuning and resonance width functions already derived. The criterion for an adiabaticity threshold can be found by equating the speed with which the island centre is changing with amplitude to the rate of particle amplitude change due to the resonance.

The rate of movement of the islands can be found from equation 5.19)

$$\frac{d\alpha_f}{d\theta} = \frac{1}{M\ \xi\ U''(\alpha_f)}\ \frac{dQ}{d\theta} \qquad (5.47)$$

The rate of change of amplitude due to the resonance is obtained from equation 5.16) modified for M crossing points,

$$\frac{d\alpha}{d\theta} = n M^{1/2} \xi V_n(\alpha) \tag{5.48}$$

where it is assumed that sin $n\psi$ = 1, i.e. we consider a particle in an island midway between a stable and unstable fixed point.

Putting $Q = Q_o + \hat{Q} \sin Q_s\theta$ and equating 5.47 and 5.48 the maximum rate of change of tune gives

$$\frac{\hat{Q}\, Q_s}{M\, \xi\, U''(\alpha_f)} \leq nM^{1/2} \xi\, V_n\,(\alpha_f)$$

i.e.

$$Q_s \leq \frac{n\, \xi^2 M^{3/2} V_n(\alpha_f)\; U''(\alpha)_f}{\hat{Q}} \tag{5.49}$$

This is evaluated for the same paramters as previously and with a beam-beam tune shift of 3×10^{-3} per intersection in the following table. f_c is the frequency in Hz.

x/σ	α_f	Q_s	f_c (Hz)
2	2	1.1 x 10-5	0.48
3	4.5	1 x 10-4	4.4
4	8	3.5 x 10-4	15.4

Table 2

We see that the critical capture frequency is more than an order of magnitude lower than the synchrotron frequency (~ 300 Hz) so this process cannot be driven by energy oscillations. However, the critical frequency falls in a range where power supply ripple can become important and it has been observed experimentally that the antiproton lifetime is very sensitive to low-frequency power supply ripple.

6. PRACTICAL IMPLICATIONS

The preceeding discussion of the single and multiresonance models of the beam-beam interaction was intended to introduce the reader to some of the basic physical phenomena involved without any pretentions of producing a precise predictive theory. Nevertheless, some of the intuitive understanding gleaned from these models has been of practical importance.

6.1 The effect of tune modulation

It is hopefully by now perfectly evident that tune modulation is bad. Figure 10 illustrates how such modulation shows up on the Schottky scans. The upper trace is the Schottky signal from a debunched proton beam, giving the usual information about the tune and the chromaticity. The lower trace shows the equivalent signal from a bunched beam. In this case the central line should be very narrow, due only to the amplitude dependence of the tune. The broadening of this line is due to low frequency ripple of the quadrupole power supplies. In this case the width is around 40Hz, corresponding to a tune ripple of $\pm 4.5 \times 10^{-4}$.

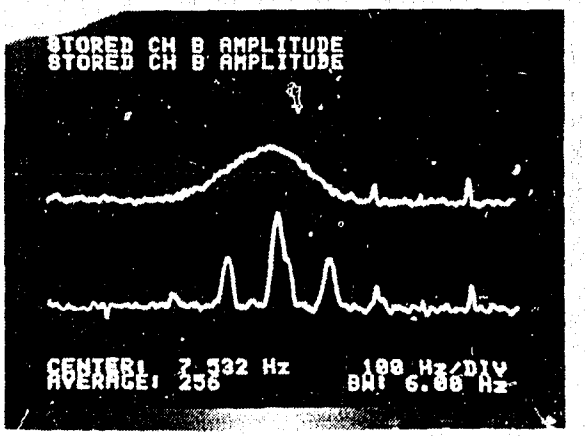

Fig. 10

Schottky signal of a betatron line for a debunched (upper) and bunched (lower) proton beam.

The sidebands are due to the tune modulation through the non-zero chromaticity and are separated by the synchrotron frequency. The amplitude of the sidebands depends on the value of the chromaticity, which is normally adjusted to be as close to zero as possible, but alway slightly positive (~ 0.1) in order to stabilise the lowest head-tail mode.

As already mentioned it was expected that low frequency ripple would be very destructive to the antiproton lifetime and experimentally this has been shown to be the case. Consequently, a considerable effort has been put into improving the power supply stability with the result that the measured width of the Schottky lines is now around 15Hz, corresponding to a tune modulation amplitude of $\pm$ 1.7 x 10^{-4} and a current stability of 6 ppm.

6.2 The Antiproton Emittance

In all the examples treated in the previous sections the small amplitude phase space is invariably stable. This is clearly due to the linearity of the beam-beam force for small emittance particles.

Up to now the SPS has always operated in the weak-strong régime with the antiproton bunch intensity approximately an order of magnitude less than that of the protons. In addition the cooled antiproton beam emittance in the accumulator is close to its design value of about 5 x 10^{-6} πrad.m, whereas the proton emittance is of the order of 15π x 10^{-6} rad.m. Therefore, in order to make use of the fact that the small amplitude phase space is stable, a considerable effort has been made to reduce the emittance dilution of the antiprotons during transfer between the accumulator and the SPS.

Figure 11 shows what happens if the antiproton emittance is too large. In this case a malfunction in the accumulator produced three bunches (z,y, and x) with successively larger emittance. The effect on the decay rates can easily be seen. Antiprotons whose amplitude exceeds the average dimensions of the proton beam are rapidly peeled off and the decay rate is initially high. Finally, as the proton bunches blow-up due to intrabeam scattering, the decay rates of the three antiproton bunches become equal.

Before being injected into the SPS the antiprotons are accelerated to 26 GeV/c in the CPS. Great care must be taken to reduce the injection errors into each of these machines. If the beam is not precisely injected onto the closed orbit the phase space filaments due to nonlinearities in the guide field or in the case of the SPS, the strong nonlinearity of the previously injected proton beam. In practice the injection optimisation is done in the opposite sense using protons travelling backwards from the SPS to CPS and from the CPS to antiproton accumulator. The tolerance requirements for this operation can be relaxed by using active damping - detecting the injection errors and correcting them with an active feedback system. A damping system for the CPS is under study and a system installed in the SPS has already given encouraging results.

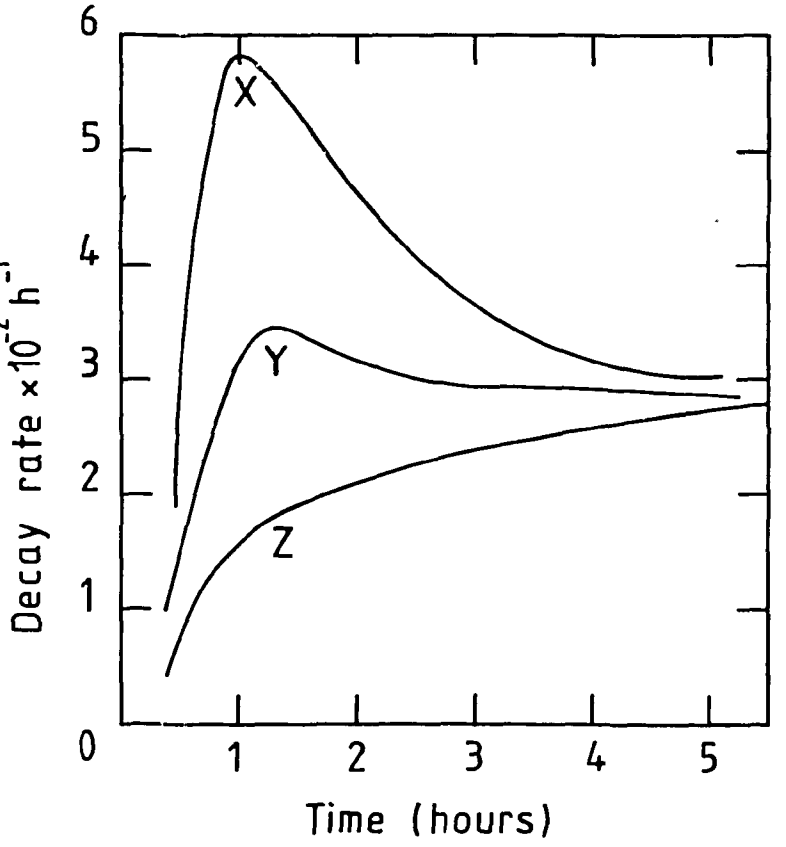

Fig. 11

Decay rates of three antiproton bunches with different emittances. The normalized emittances $E = \varepsilon\beta\gamma/\pi$ were $E_x = 17$, $E_y = 15$, $E_z = 12$. The proton emittance $E_p = 16$ and $\xi = .004$.

Another source of emittance dilution is the mismatch of dispersion and betatron functions between the different machines. The dispersion matching between the CPS and SPS is especially important because of the large momentum spread in the beam (± 0.3%). A lot of effort has been devoted to measuring the dispersion function at the CPS extraction using a 'probe' antiproton beam with a very small momentum spread. The results of these measurements have been used to finely tune the beam optics between the CPS and SPS. When the whole chain is carefully optimised, an overall emittance blowup of less than a factor of two between accumulator and SPS stored can be achieved.

Clearly as the intensity of the antiprotons increases towards that of the protons the advantage of unequal emittances will disappear.

6.3 The Need for Bunch Separation

In order to reach design luminosity the SPS is required to store 6 proton and 6 antiproton bunches. This would result in 12 interactions per revolution. According to the theory outlined above, the resonance excitation would be increased by something like a factor of $\sqrt{2}$ but the total tune spread would be doubled. It would then be no longer possible to keep clear of the 10th order resonances. In fact, an experiment with 6 proton bunches colliding with a single antiproton bunch has shown that the antiproton bunch lifetime is reduced by about a factor of 4 compared with the 3-bunch case, which is clearly unacceptable. This means that in order to accommodate 6 bunches per beam they must be separated at the unwanted collisions. Another reason that separation is desirable is to eliminate the tune modulation and excitation of odd order resonances due to the crossings at non-zero dispersion. A scheme to achieve this using electrostatic separators has been proposed 28] and some prototype hardware is being installed. An accurate compensation of the deflections will be needed to make the beams collide head-on at the useful intersections. An experiment has shown that a residual displacement of 0.2σ between the beams halves the lifetime.

7. CONCLUSIONS

Up to now the SPS has operated in the weak-strong régime with a beam-beam tune shift per intersection of up to 4×10^{-3} for the antiprotons and with 6 intersections per revolution. Strong beam-beam effects are observed and limit the working space in the tune diagram to a very small region which is free from tenth order resonances. Further increase in tune spread as a result of increasing the number of bunches from three to six reduces the antiproton beam lifetime to an unacceptable value so beam separation in the unwanted intersections will be required.

At the present time, good use is made of the fact that the weak antiproton beam has a substantially smaller emittance than the proton beam. As the antiproton beam intensity increases the proton beam will start to be affected by the beam-beam force and it is unlikely that the collider will be able to operate with as good a beam lifetime as presently achieved (~ 40 hours for the antiprotons) and with such a high tune shift parameter. The choice then will be either to reduce the linear tune shift (and thereby the peak luminosity) or to fill the machine much more frequently as is the case for e^+e^-machines. The second alternative will clearly require a much faster accumulation rate of antiprotons.

The theories outlined in this report are clearly of limited predictive value. Nevertheless, they provide a qualitative understanding of a number of experimentally observed phenomena. Finally, it is hoped that the discussion has served to improve the comprehension of the non-specialist of the complexities of the beam-beam interaction.

8. ACKNOWLEDGEMENTS

I have benefitted from many discussions on the subject of the beam-beam interaction with a number of people, in particular with E.D. Courant, J. Gareyte, M. Month, S. Peggs and J. Tennyson. I would also like to thank W. Middelkoop for reading the manuscript and E. Kaiser for putting it all together.

REFERENCES

1. M. Month and J.C. Herrera, eds, Nonlinear Dynamics And The Beam-Beam Interaction, AIP Conference Proceedings, No. 57, (1979).
2. Proceedings of the Beam-Beam Interaction Seminar, SLAC-PUB-2624 (1980).
3. A. Chao, A Summary Of Some Beam-beam Models, reference 1, p 42.
4. S. Kheifets, Experimental Observations and Theoretical Models for Beam-Beam Phenomena, SLAC-PUB-2700, (1981).
5. J. Schonfeld, The Effects Of Beam-Beam Collisions on Storage Ring Performance - A Pedagogical Review, Fermilab-Conf-83/17-THY, (1983).
6. J. Seeman, SLAC-PUB-3182, (1983).
7. A. Piwinski, DESY 83-028, (1983).
8. A. Piwinski, Proc. 11th Int. Conf. on High-Energy Acceleratoas, 751, (1980).
9. S. Peggs, R. Talman, ibid, 754, (1980).
10. S. Myers, IEEE Trans. Nucl. Sci., NS-28, 2503, (1981).
11. A. Hofmann, et al. Proc. 11th Int. Conf. on High-Energy Accelerators 713, Geneva, (1980).
12. L. Evans, J. Gareyte, CERN SPS/82-8 (DI-MST), (1982).
13. E. Keil, International School of Particle Accelerators, CERN 77-13, p. 314, Erice, (1977).
14. J. le Duff, Ibid. p. 377
15. E.D. Courant, H.S. Snyder, Ann. Physics 3, p 1, (1958).
16. A. Schoch, CERN 57-21, (1958).
17. G. Guignard, CERN 78-11, (1978).
18. N. Bogoliubov and Y. Mitropolsky, Asymptotic Methods In the Theory of Nonlinear Oscillations, Hindustan Publishing Corpn. Delhi, (1961).
19. L. Evans, SPS/DI(MST) Note/81-2, (1981).
20. A.C. Ruggiero, L. Smith, 1973 PEP Summer Study.
21. A. Month, BNL 19533, (1975).
22. S. Peggs, Private Communication, (1983).
23. B. Chirikov, Physics Reports, 52, 263, (1979).
24. J. Tennyson, in Physics Of High-Energy Particle Accelerators, AIP Conf, Proceedings No. 87, 345, (1981).
25. E.D. Courant, ISABELLE project tech. note No. 163, (1980).
26. A.W. Chao, M. Month, BNL 18860, (1974).
27. M. Month, BNL 19583, (1975).
28. L. Evans, A. Faugier, SPS/DI-MST/Note 83-1, (1983).